

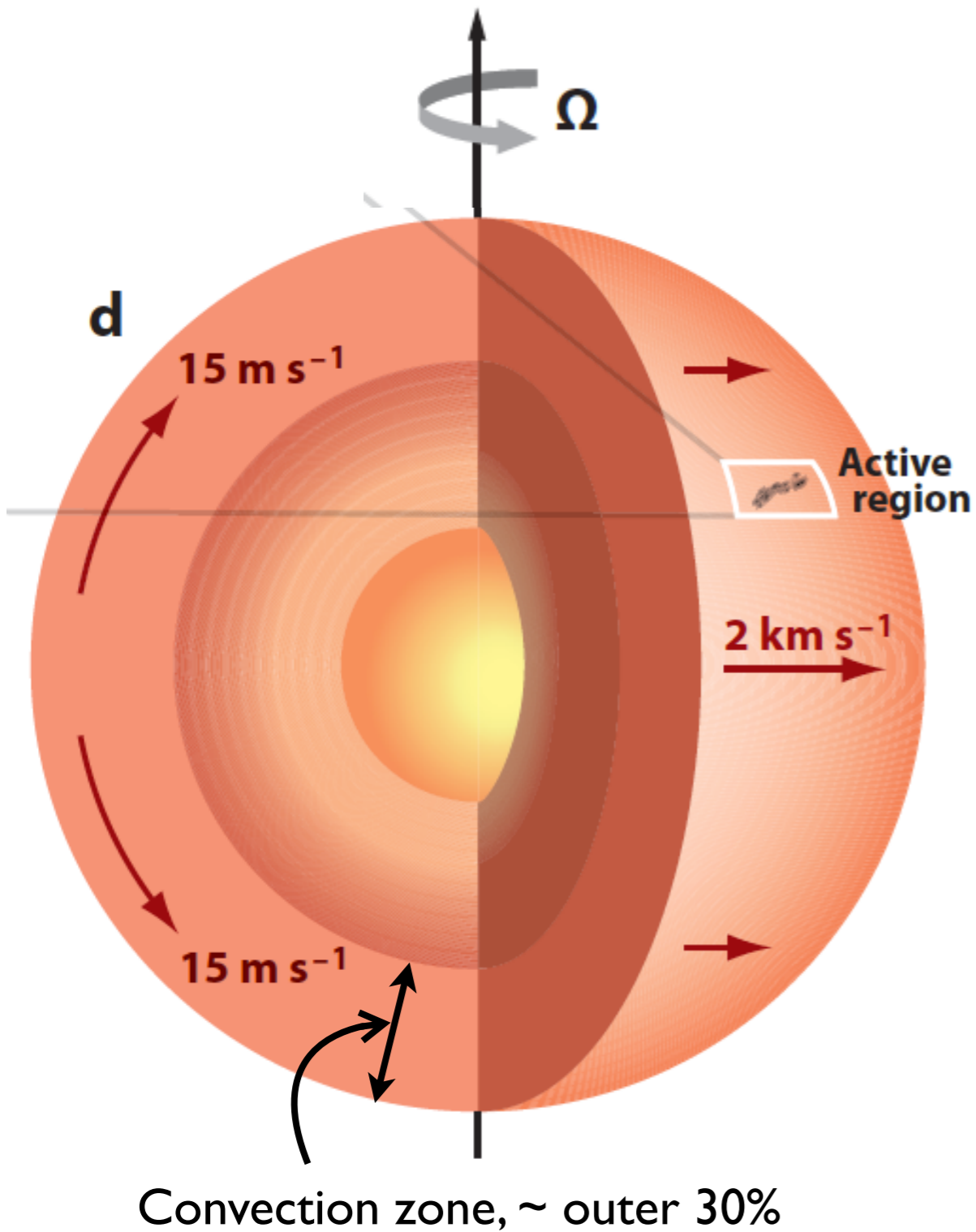
Meridional Circulation on the Sun: Helioseismic Measurements and Implications for Interior Dynamics

S.P. Rajaguru

(Indian Institute of Astrophysics, Bangalore)

Collaborator: H.M. Antia (TIFR, Mumbai)

Rotation and Meridional circulation



Eddington (1920) reasoned that a rotating star in radiative equilibrium should develop circulating currents along the meridians. He also suggested that such currents would lead to differential rotation, as observed on the solar surface.

Surface meridional flow has been observed using several different techniques, and is well established:

(i) from direct Doppler observations

-- Duvall 1979, Hathaway 1996, Ulrich 2010

(ii) feature tracking, e.g. magnetic elements

-- Komm et al. 1993, Hathaway and Rightmire 2010

(iii) local helioseismology

-- e.g., Basu and Antia 2010

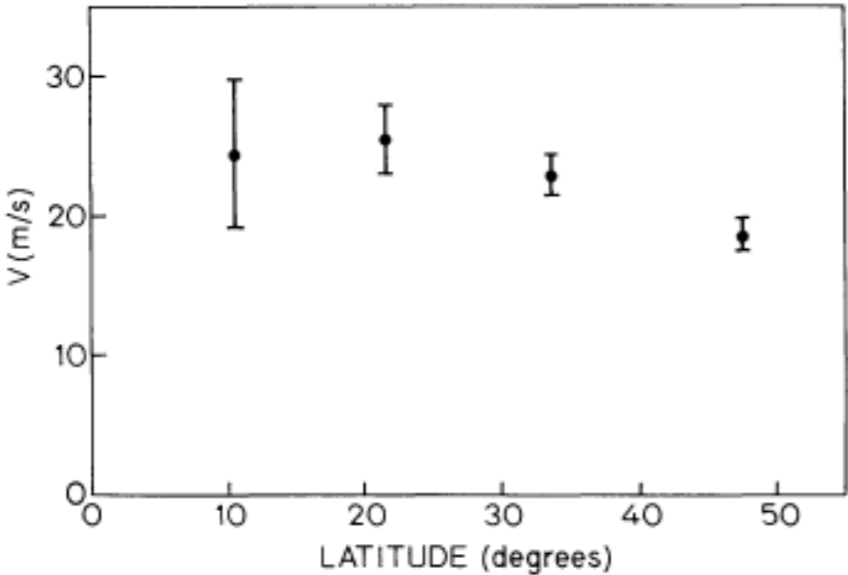
An early observation from direct Doppler observations:

LARGE-SCALE SOLAR VELOCITY FIELDS

THOMAS L. DUVALL, Jr.*

Institute for Plasma Research, Stanford University, Stanford, Calif. 94305, U.S.A.

(Received 17 July, 1978; in final form 8 March, 1979)



From Dopplergrams, MWO.
Ulrich, R.K. 2010 ApJ

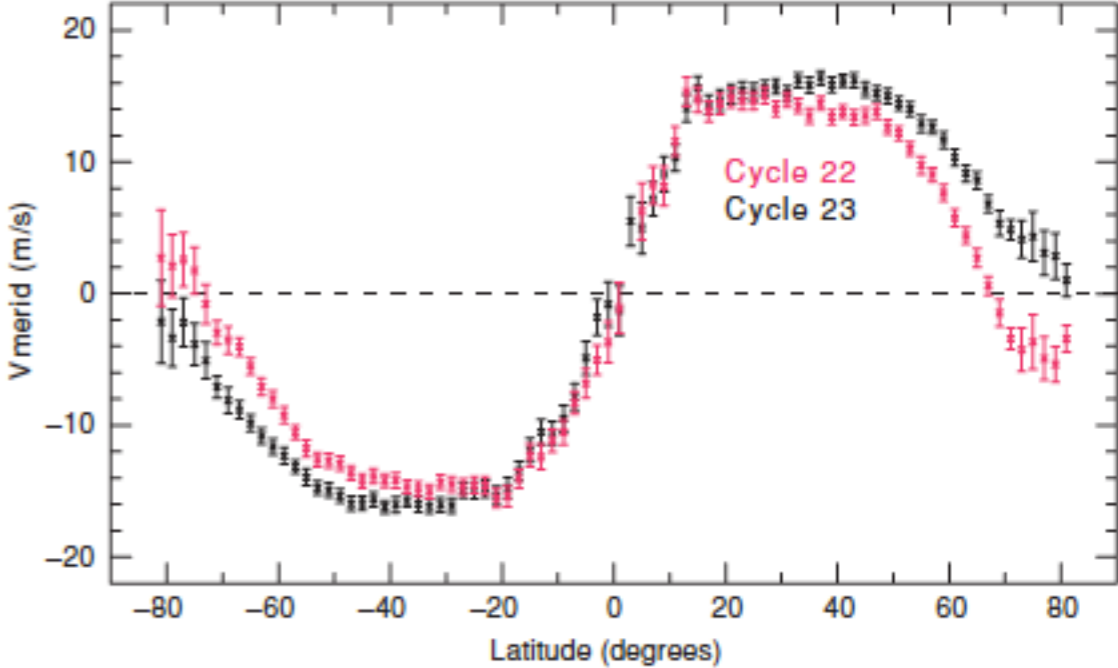
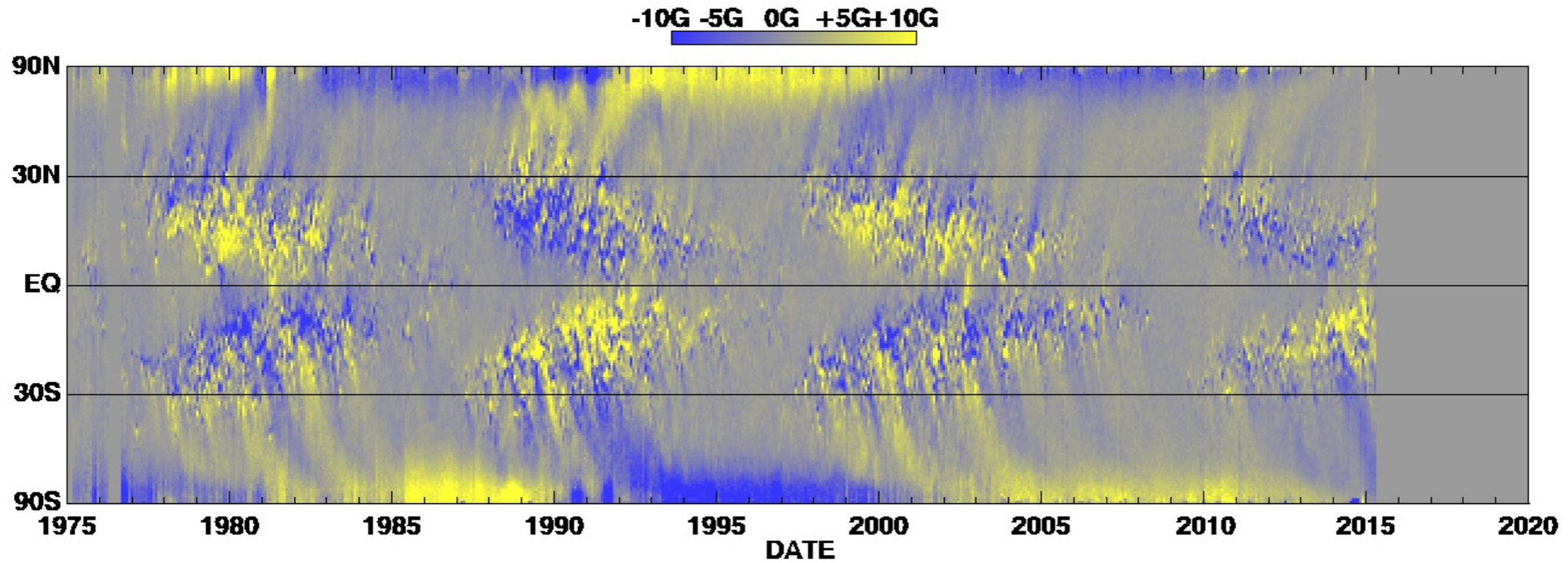
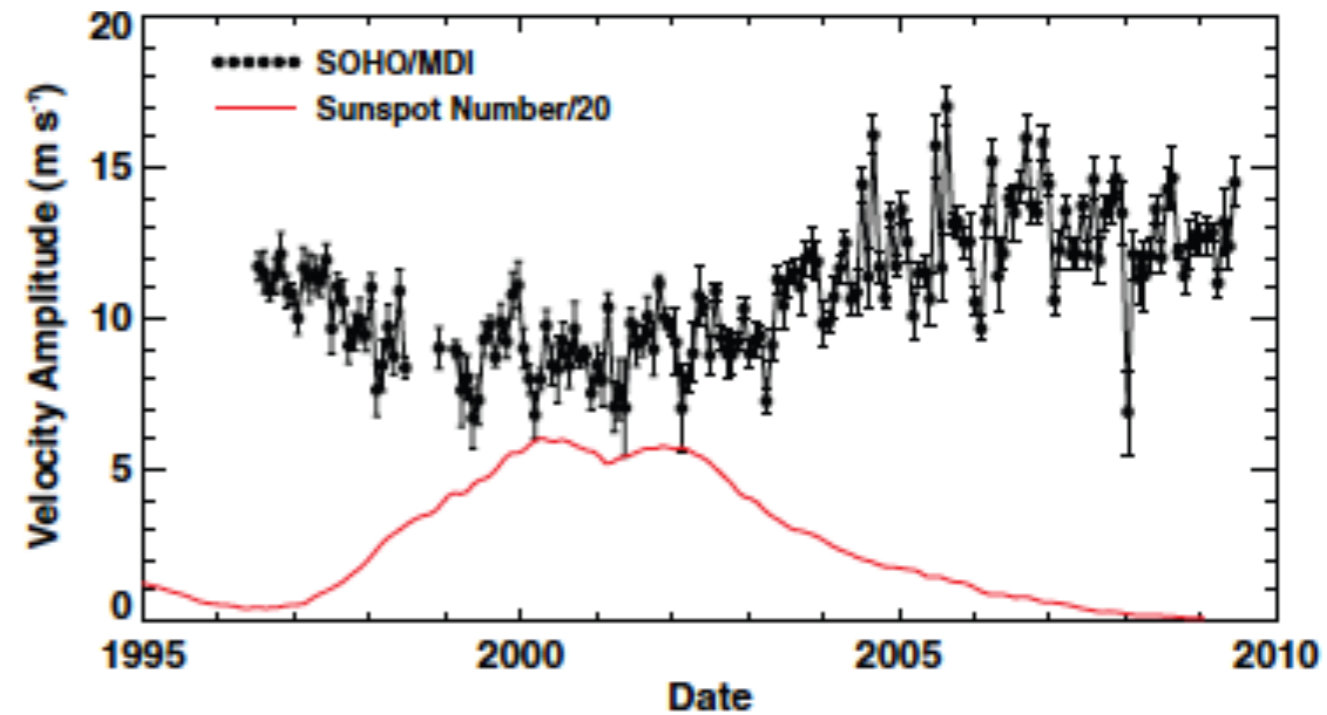
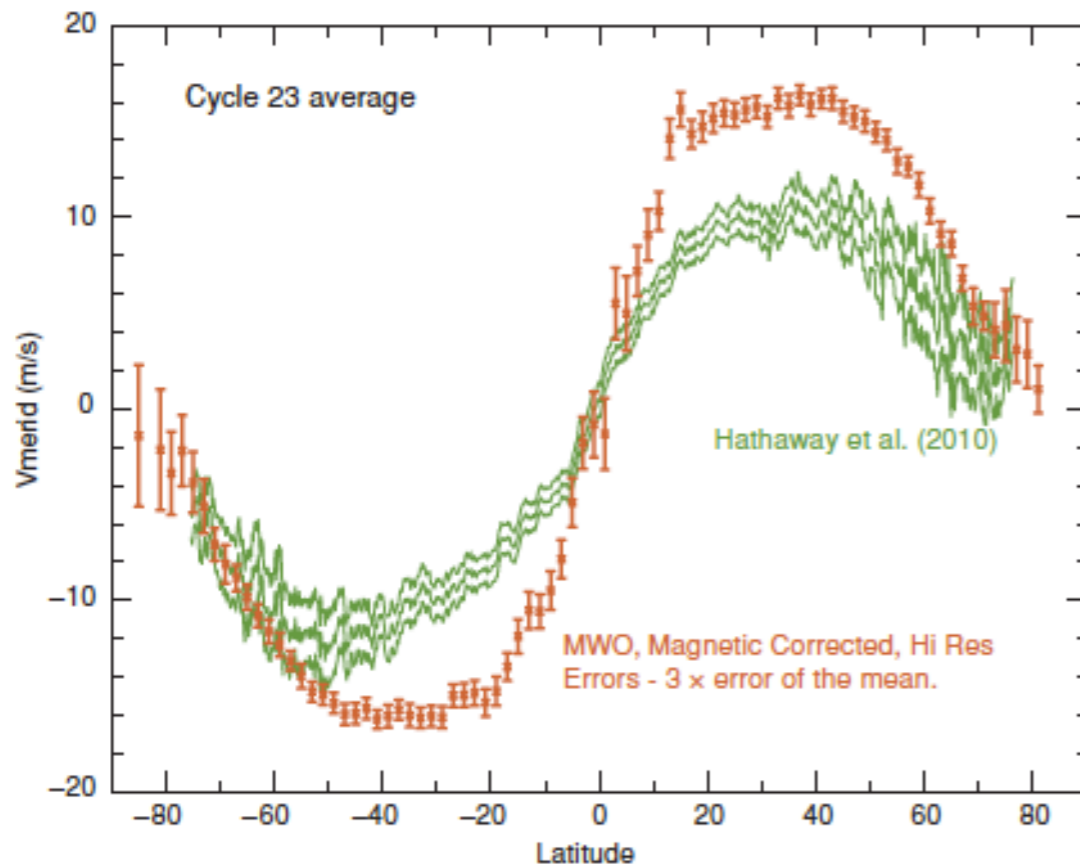


Fig. 11. Assuming the meridional flow is horizontal at the photosphere, the average symmetric component of the meridional circulation has been corrected for the projection of the velocity vector.

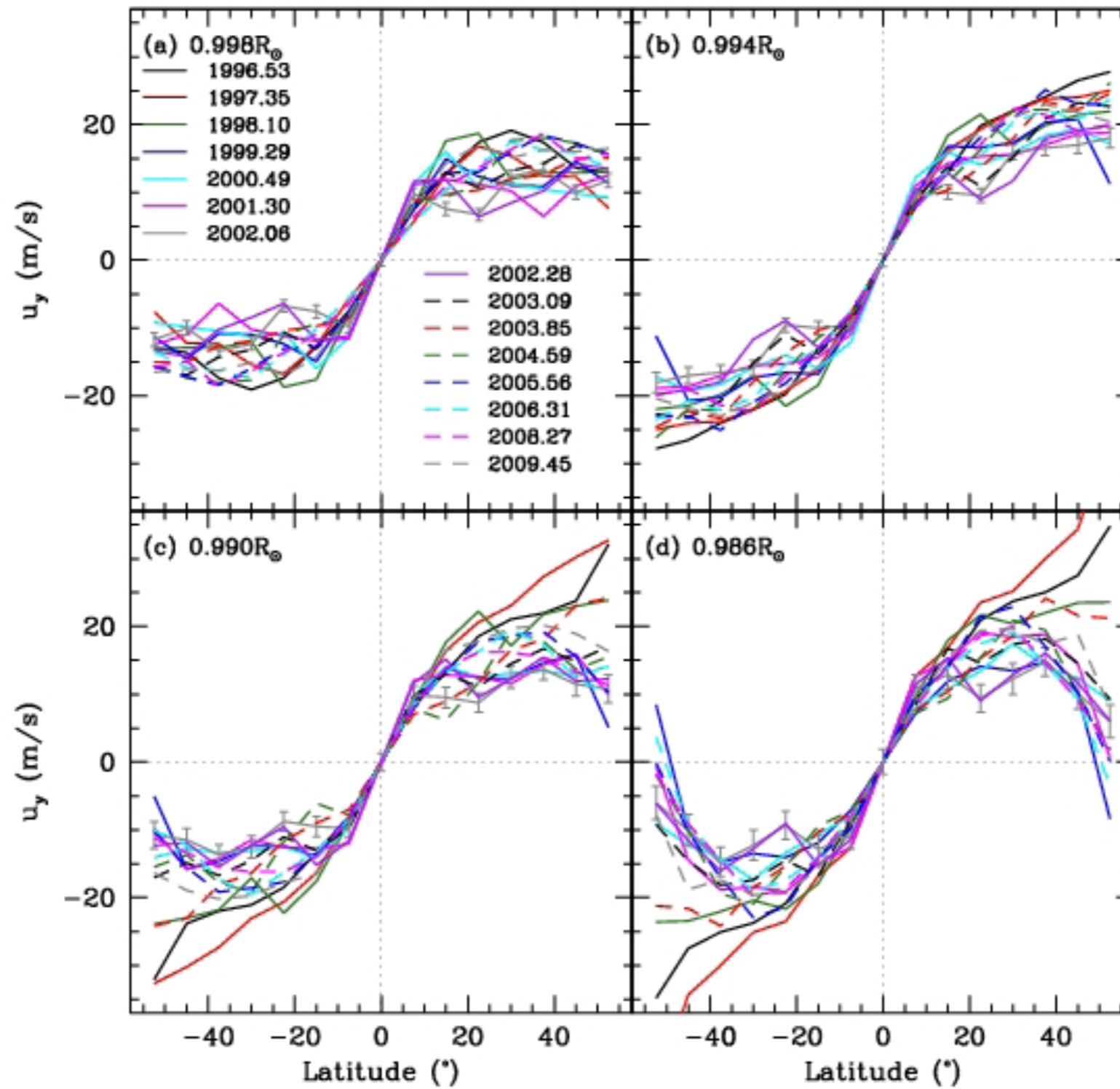
Meridional flow from magnetic feature tracking, e.g. Hathaway et al. (2010, Science)



Hathaway NASA ARC 2015/05

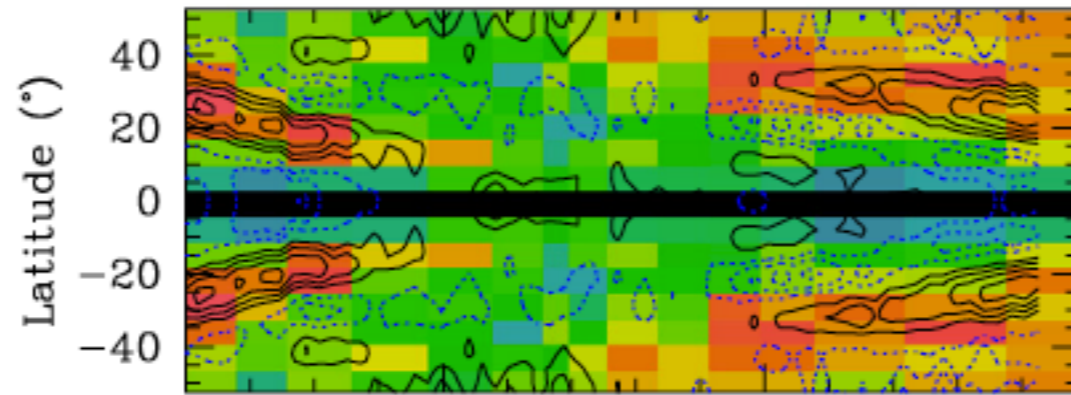
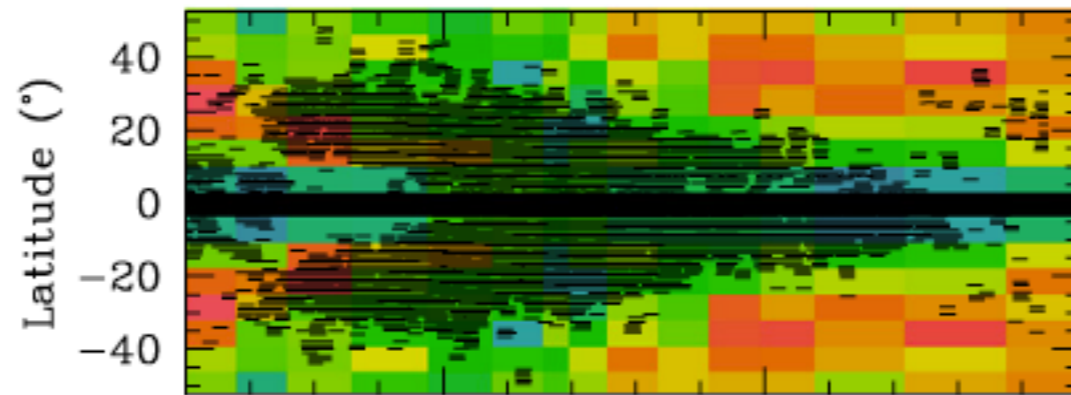


Meridional flow from ring diagram analysis (Basu and Antia 2010)

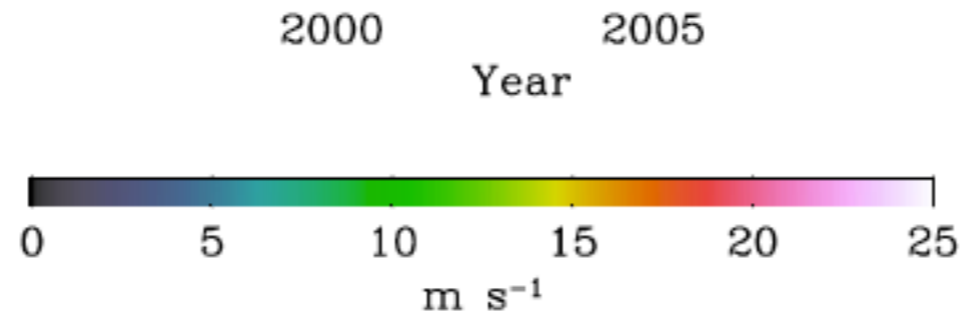


SOLAR MERIDIONAL FLOWS DURING SOLAR CYCLE 23

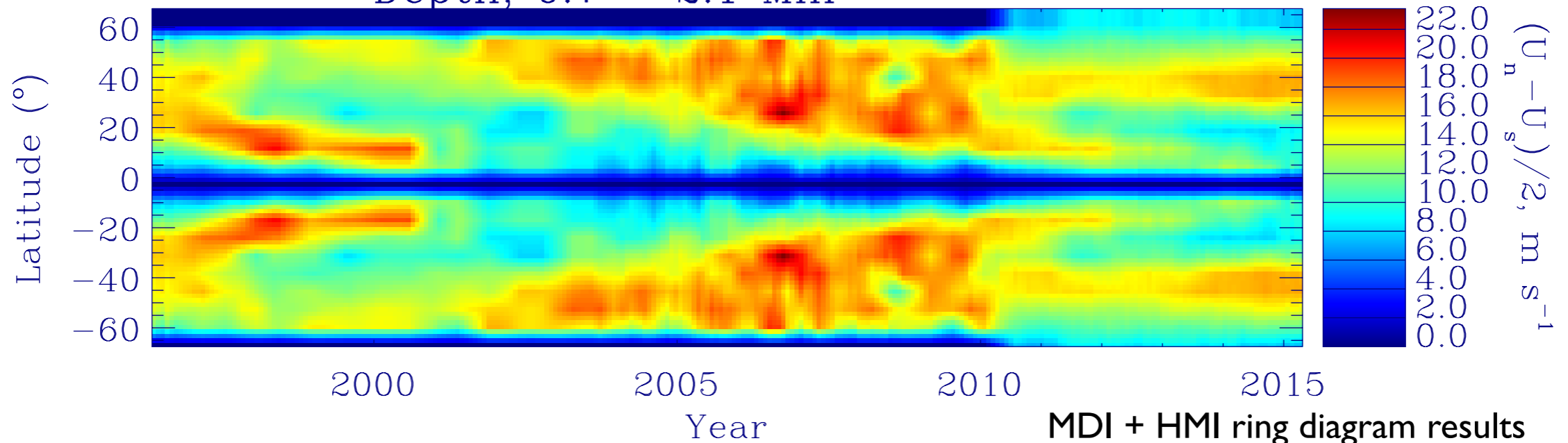
(Basu and Antia 2010)



Depth, 1.4 Mm



Depth, 0.7 – 2.1 Mm

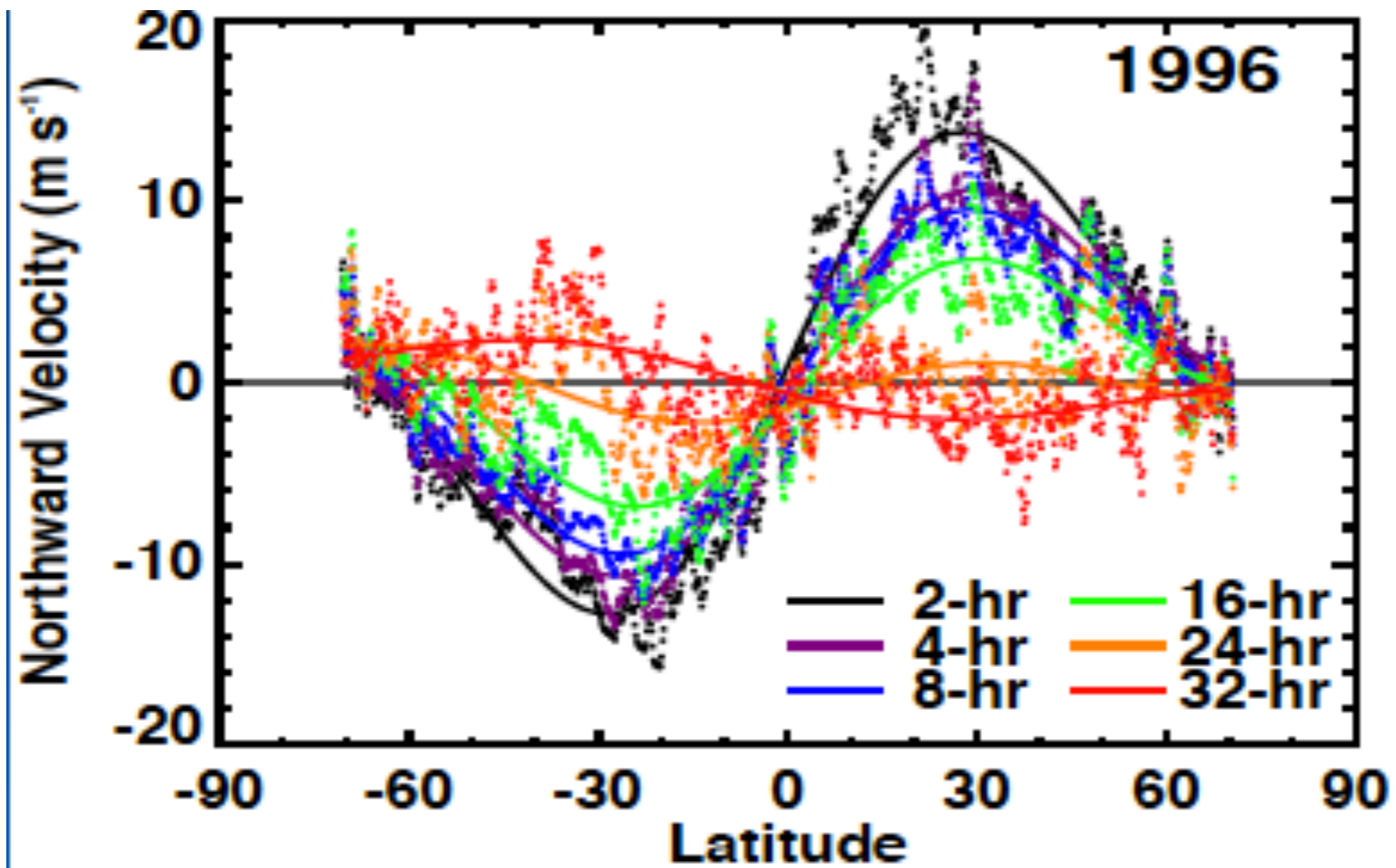


MDI + HMI ring diagram results

(Gilda and Rajaguru, work in progress)

Inferences on meridional circulation from tracking of supergranules

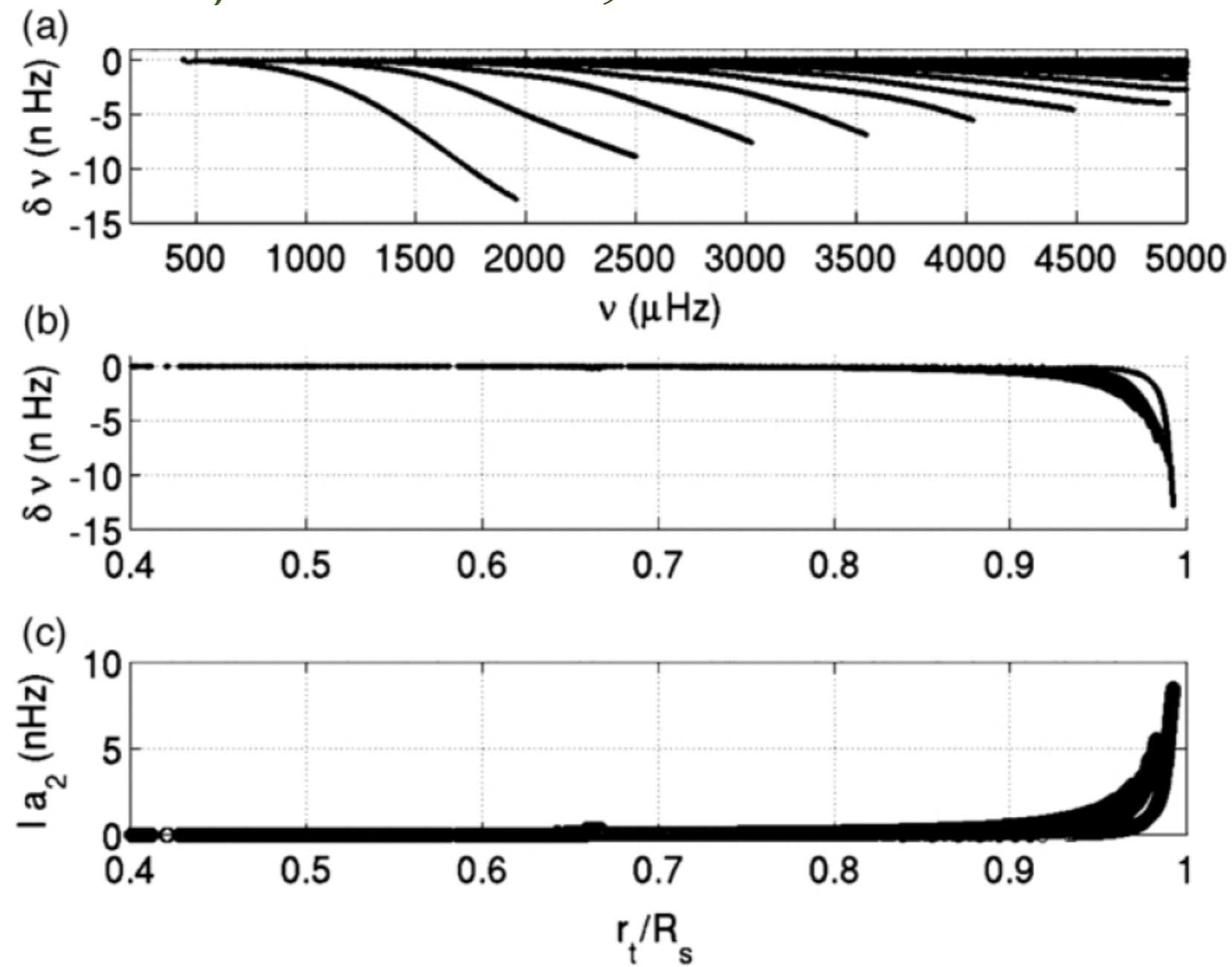
Hathaway 2012



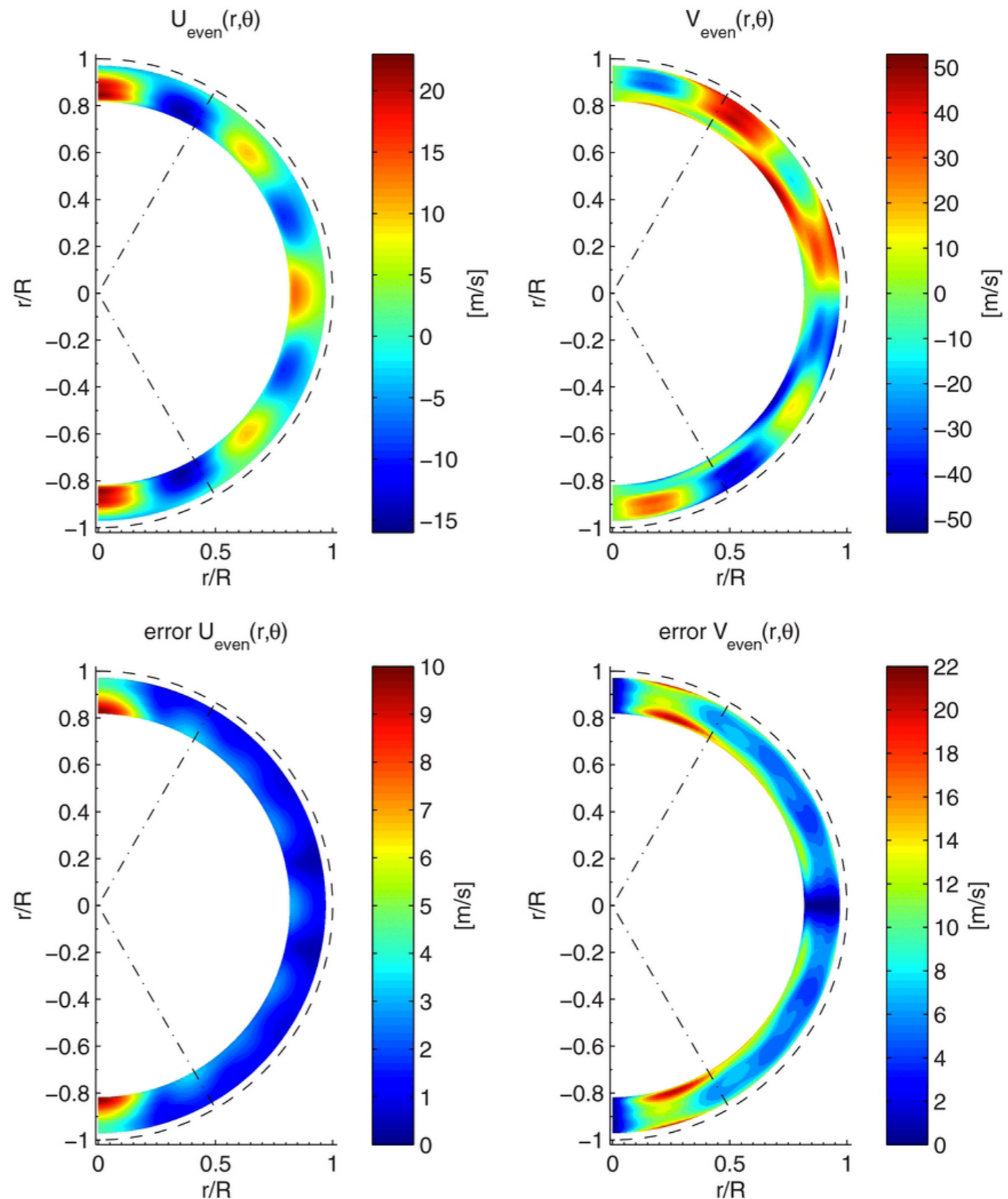
Meridional Flows from Helioseismology

To first order the contribution of meridional flow to frequencies of global modes vanishes and hence these cannot be used to infer meridional flow. Quasi-degenerate perturbation theory can be used to estimate the second order contributions due to mode coupling.

Quasi-degenerate perturbation theory is used to calculate the effect of meridional flow (Chatterjee & Antia 2009)



In general the effect of meridional flow on frequencies is small but for some pair of modes with close frequencies and neighbouring l values the effect could be large because of mode coupling, which also distorts the eigenfunction. [Schad et al. \(2013\)](#) have used this distortion in eigenfunction to infer meridional flows.



Schad et al. (2013)

Why is meridional circulation important?

Astron. Astrophys. 303, L29–L32 (1995)

The solar dynamo with meridional circulation

A.R. Choudhuri^{1,2}, M. Schüssler¹, and M. Dikpati^{2,3}

¹ Kiepenheuer-Institut für Sonnenphysik, Schöneckstrasse 6, D-79104 Freiburg, Germany

² Department of Physics, Indian Institute of Science, Bangalore - 560012, India

³ Indian Institute of Astrophysics, Bangalore - 560034, India

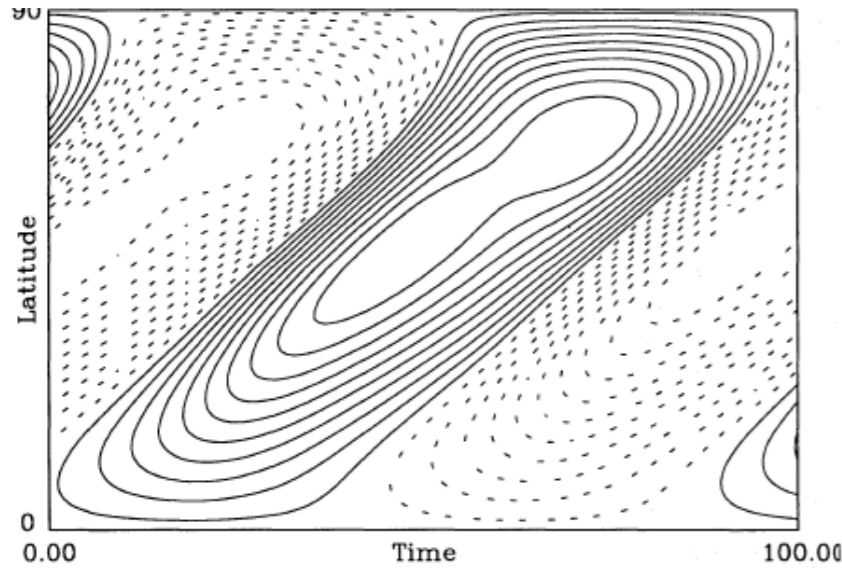


Fig. 1. Butterfly diagram for the toroidal field, taken near the bottom of the convection zone. Meridional circulation is switched off. Time is given in units of $t_0 \simeq 3.5$ years.

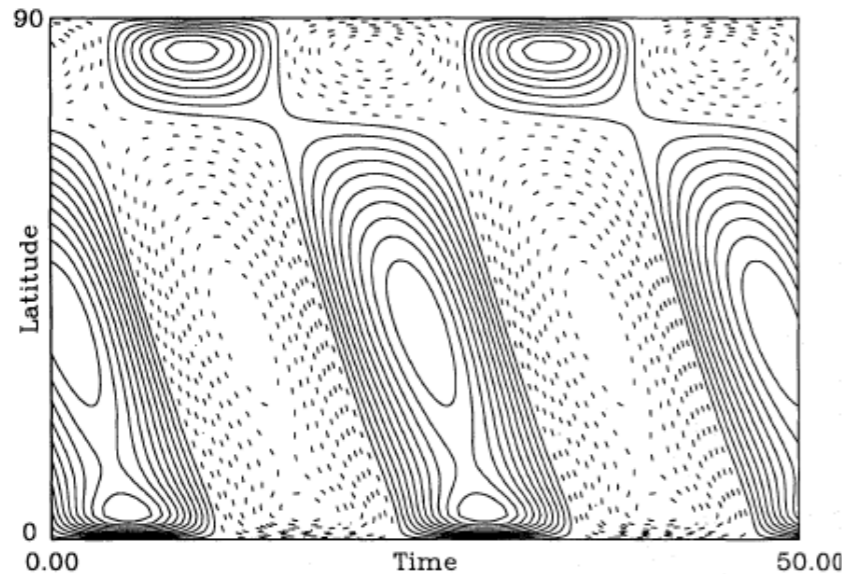
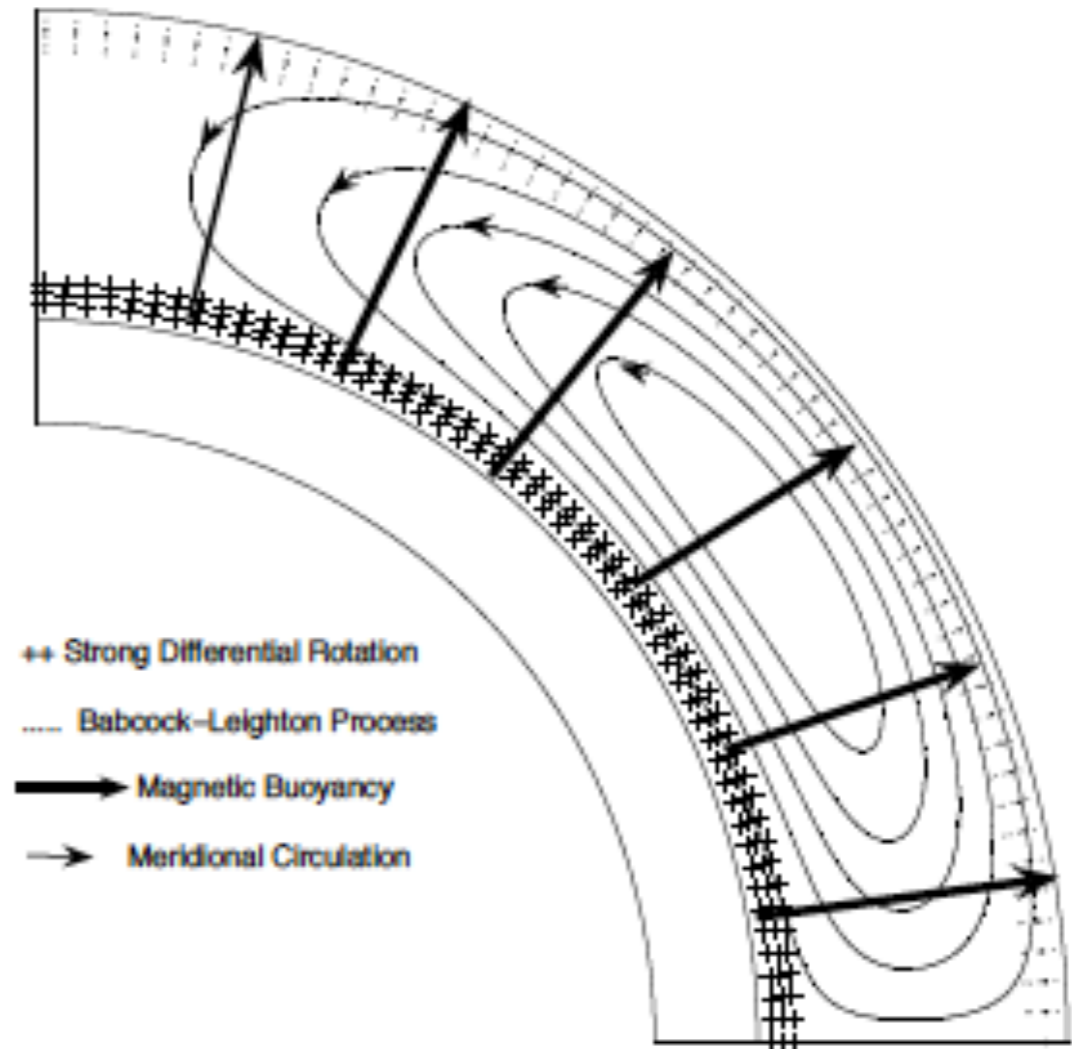


Fig. 2. Same as Fig. 1, but for the case with meridional circulation ($v_0 = 7 \text{ m}\cdot\text{s}^{-1}$). The dynamo waves now propagate equatorward and the period has decreased (note the different time interval).

Flux Transport Dynamamos



Cartoon by A.R. Choudhuri (2014)

Time-distance helioseismic measurements of meridional flow

Early measurements by Giles, Duvall et al. 1997, *Nature*, using MDI/SOHO data

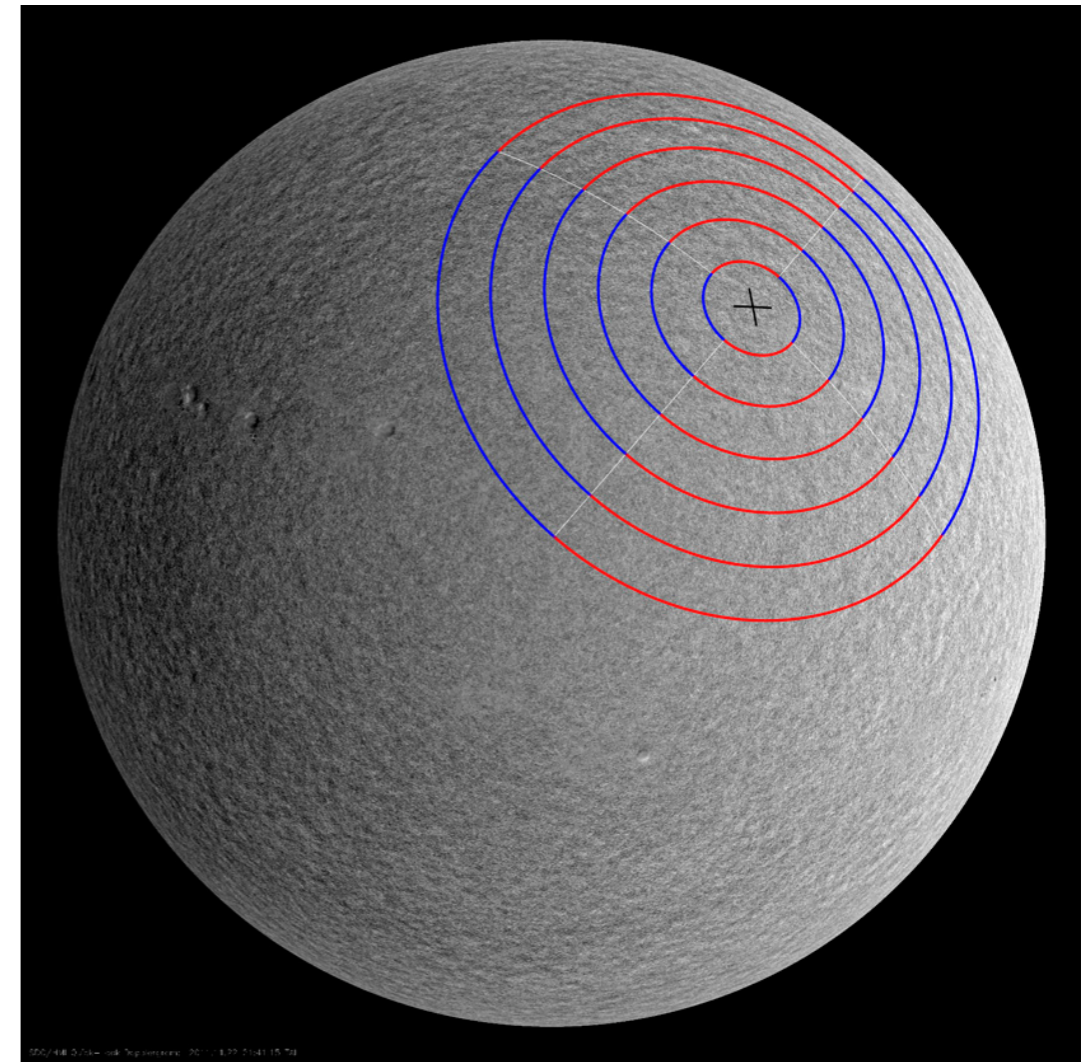
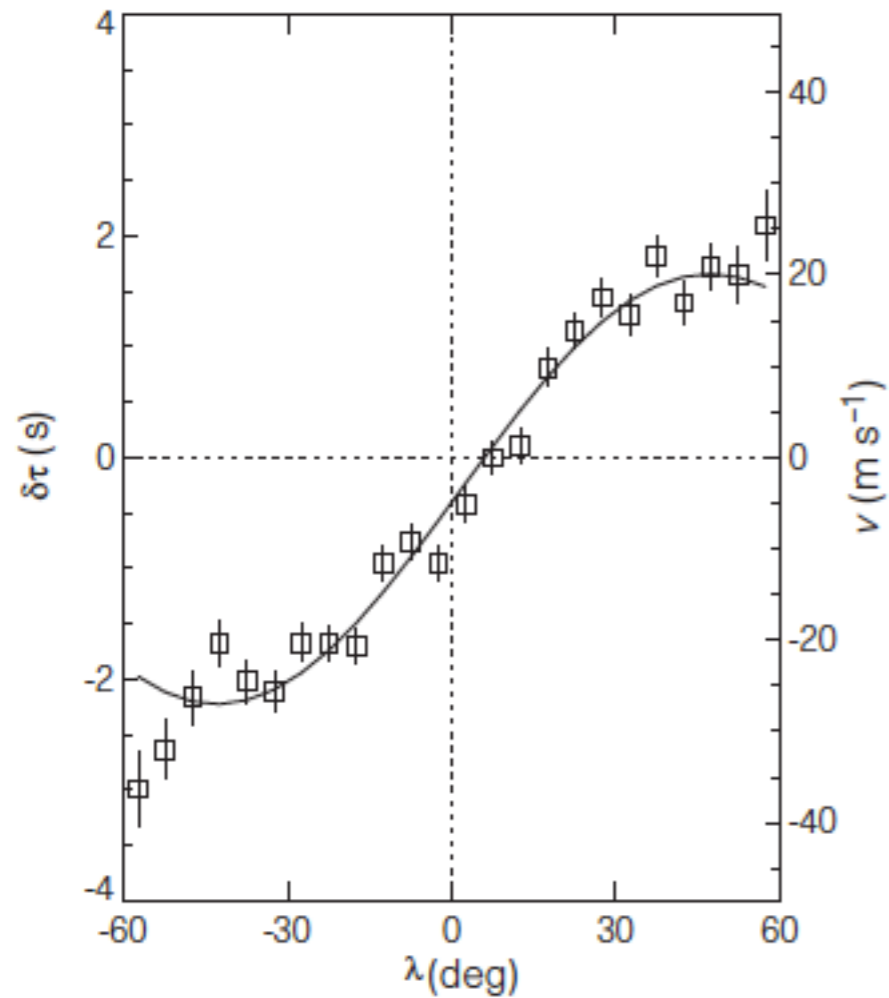
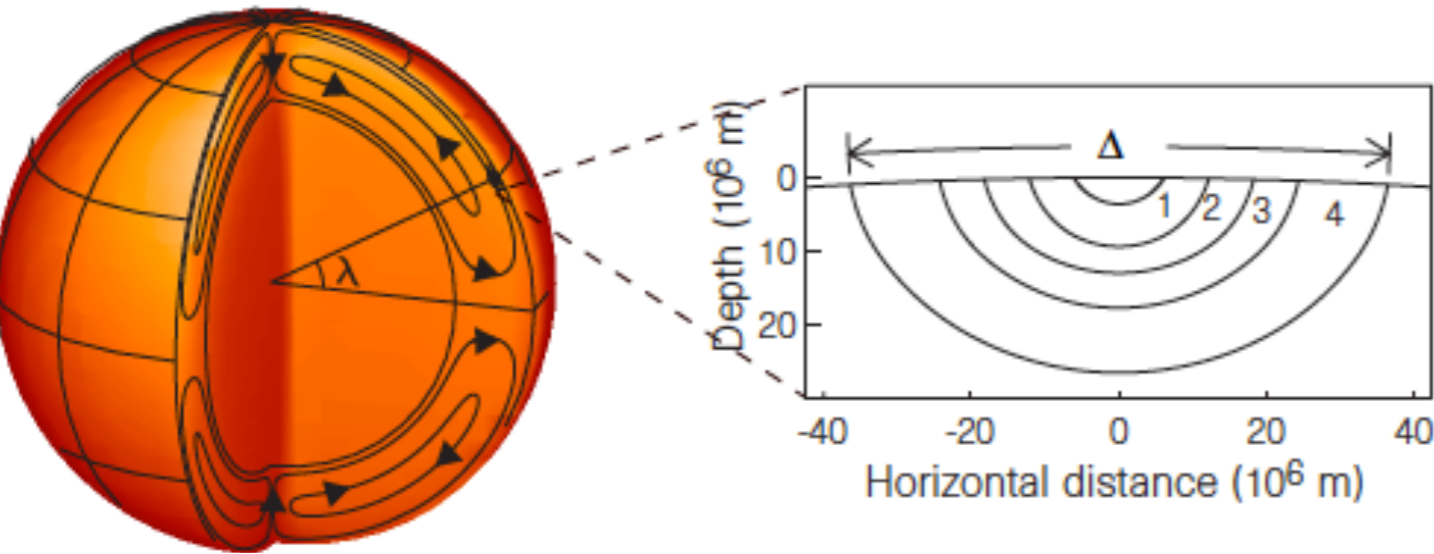


Figure Credit: Hanasoge et al. 2011

Center-to-limb Systematics in Helioseismic Travel Times

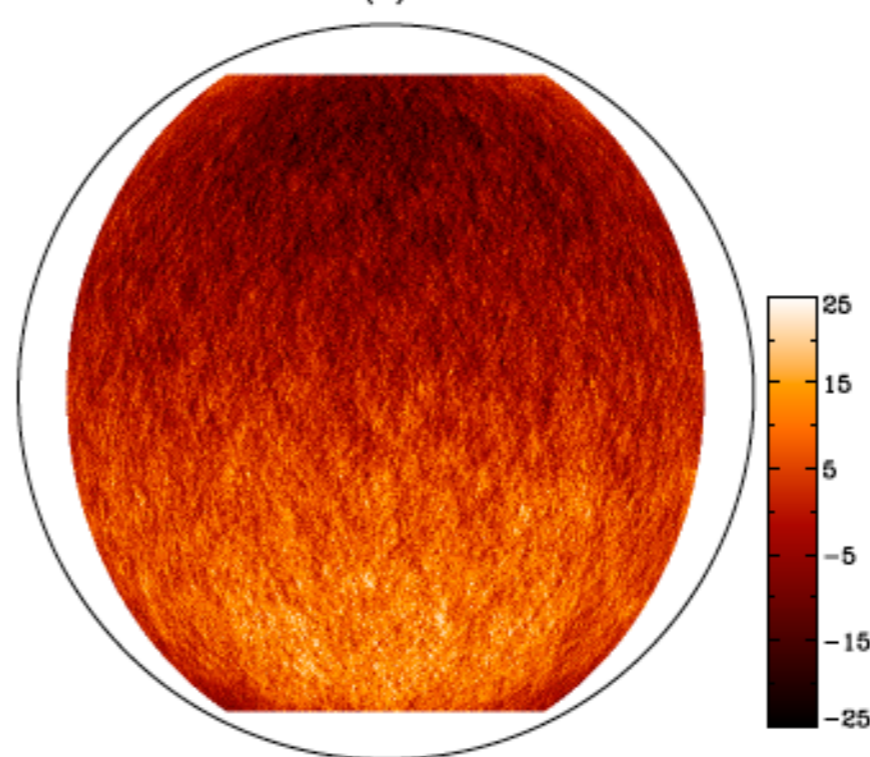
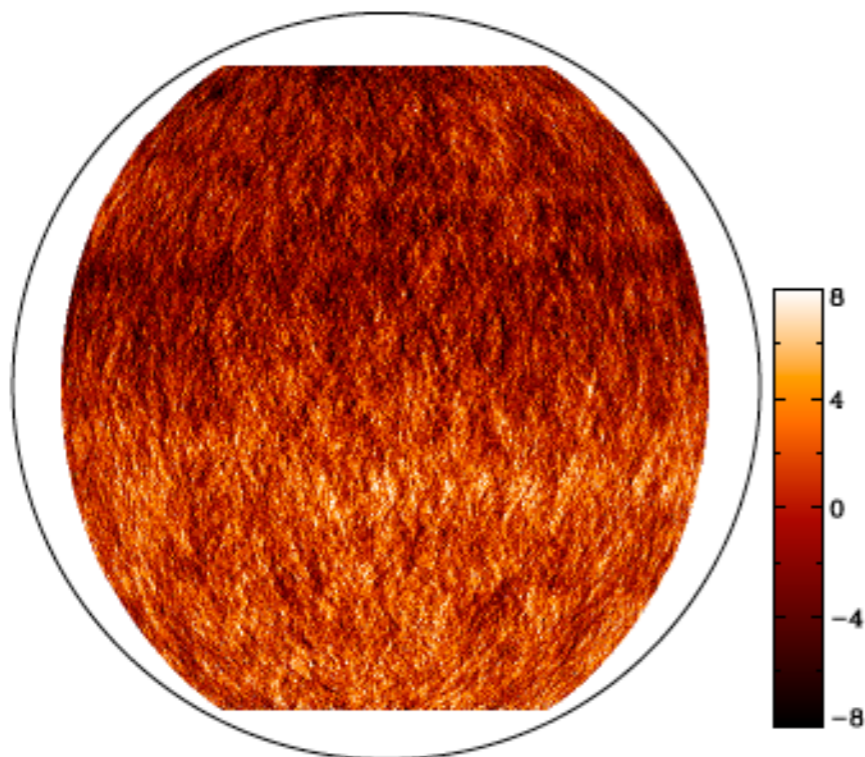
-- Zhao et al. 2012, ApJ

from HMI Doppler Velocities

from HMI continuum intensities

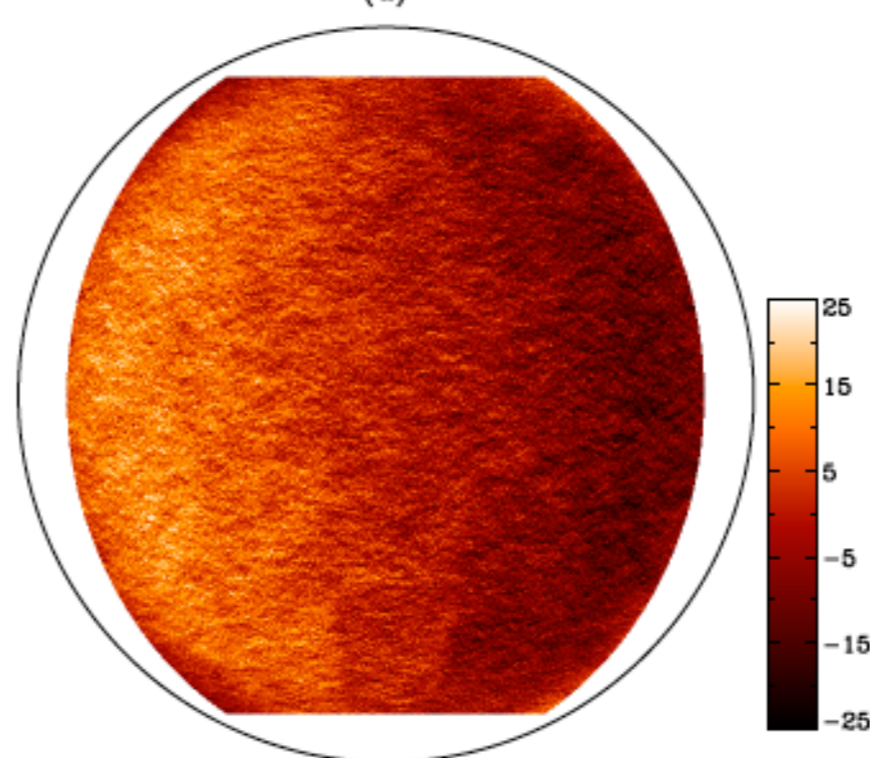
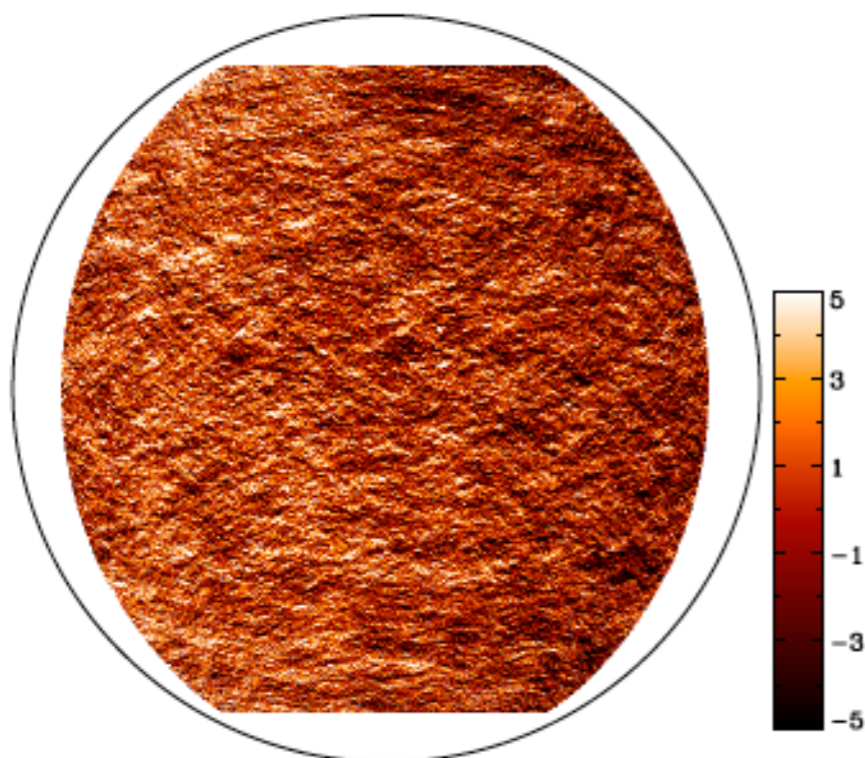
(a)

(b)



(c)

(d)



Center-to-limb Systematics in Helioseismic Travel Times

-- Zhao et al. 2012, ApJ

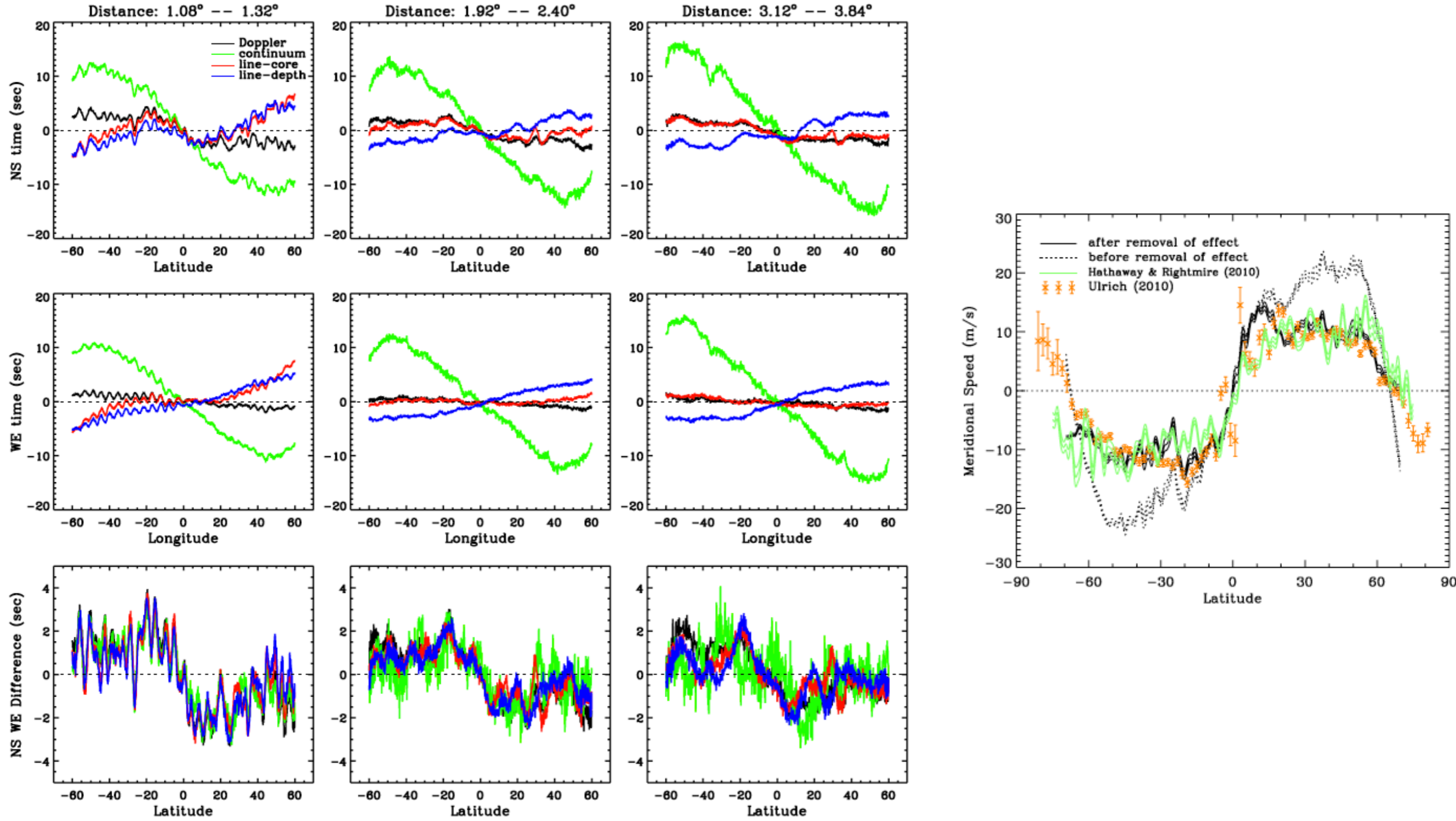
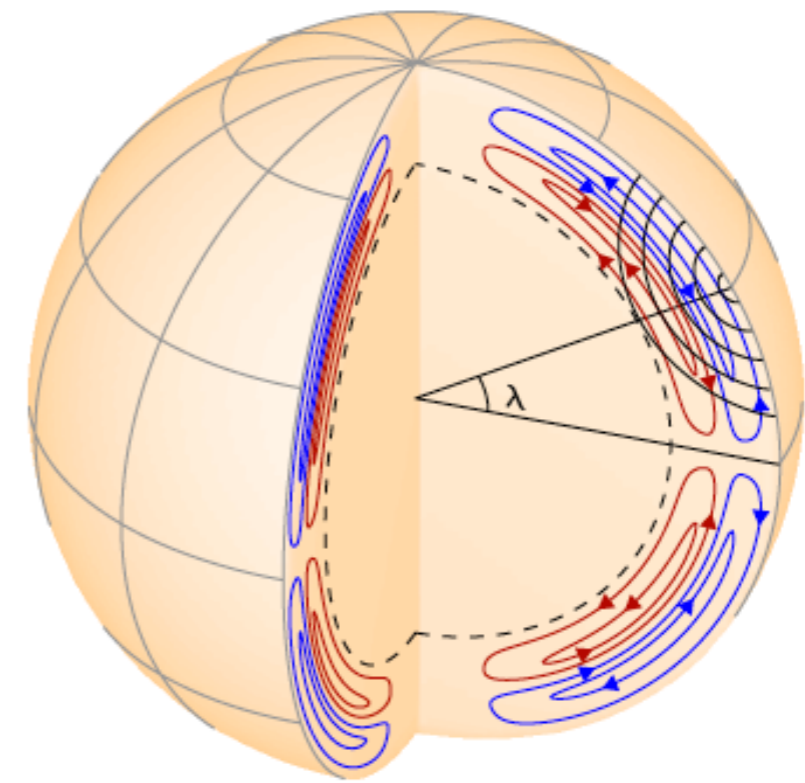
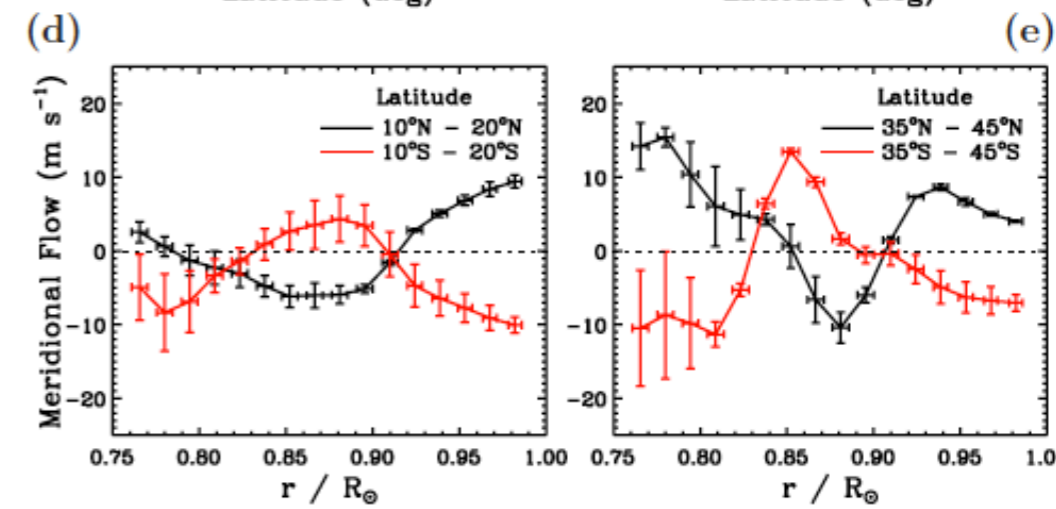
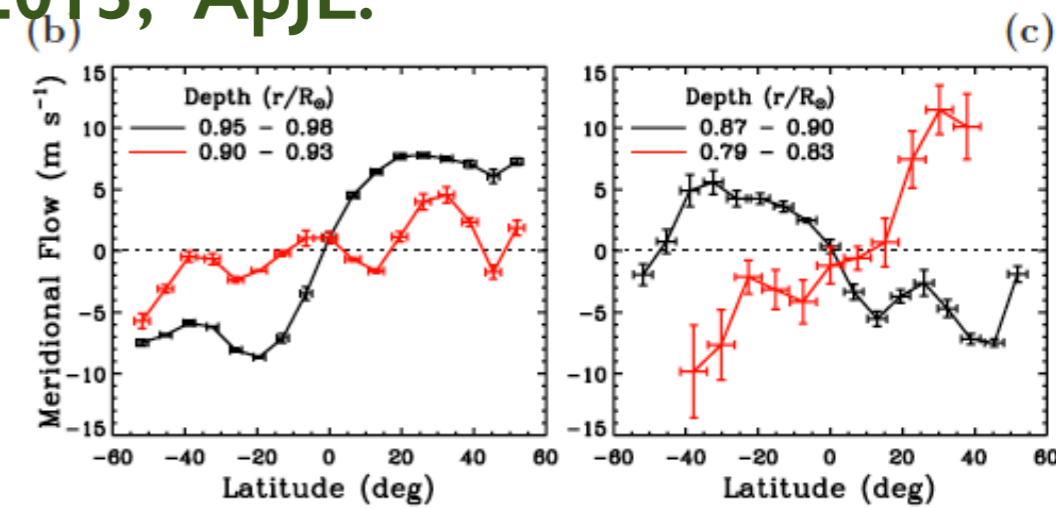
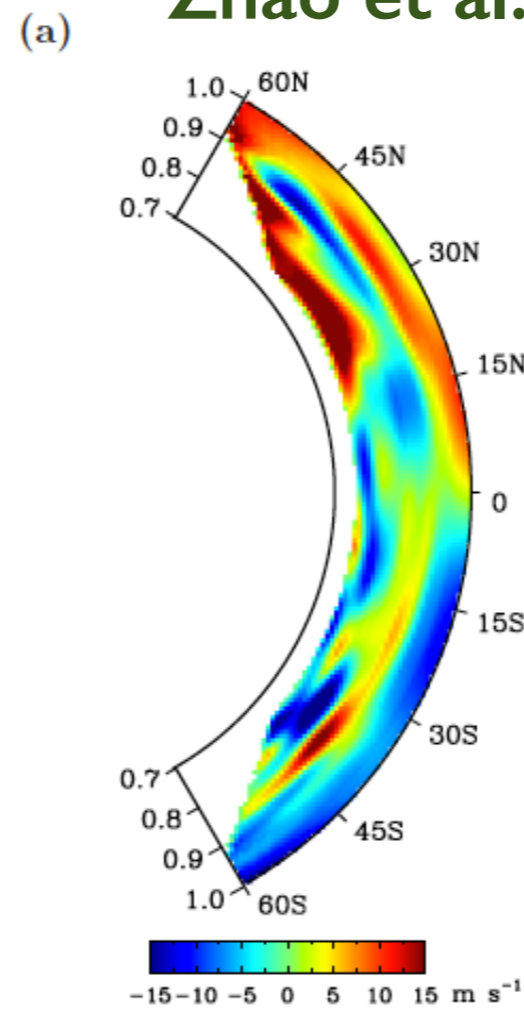
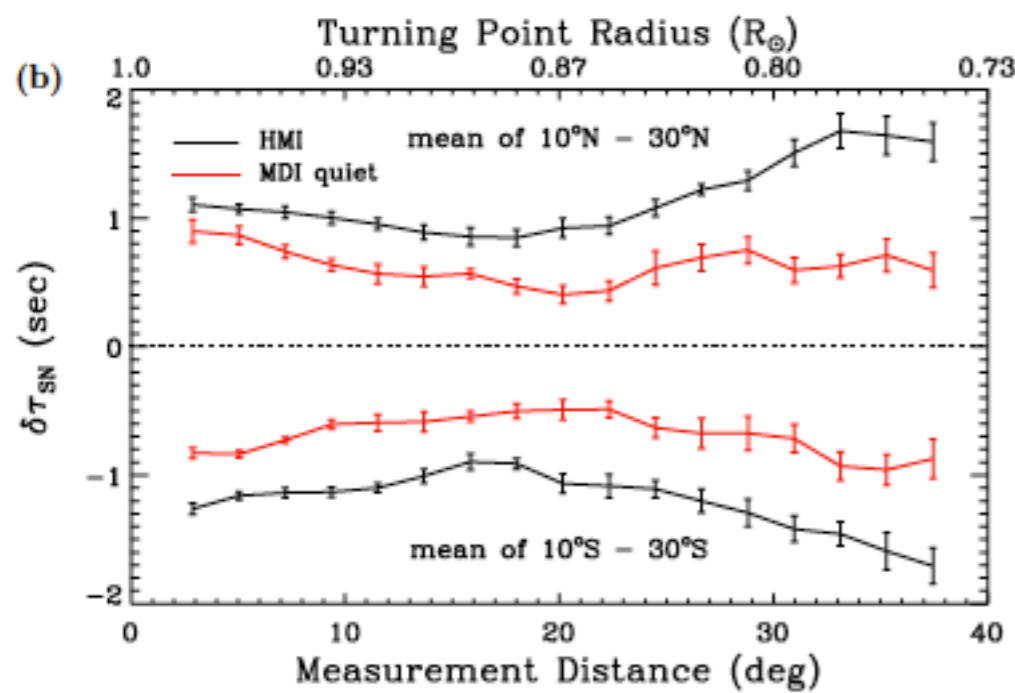
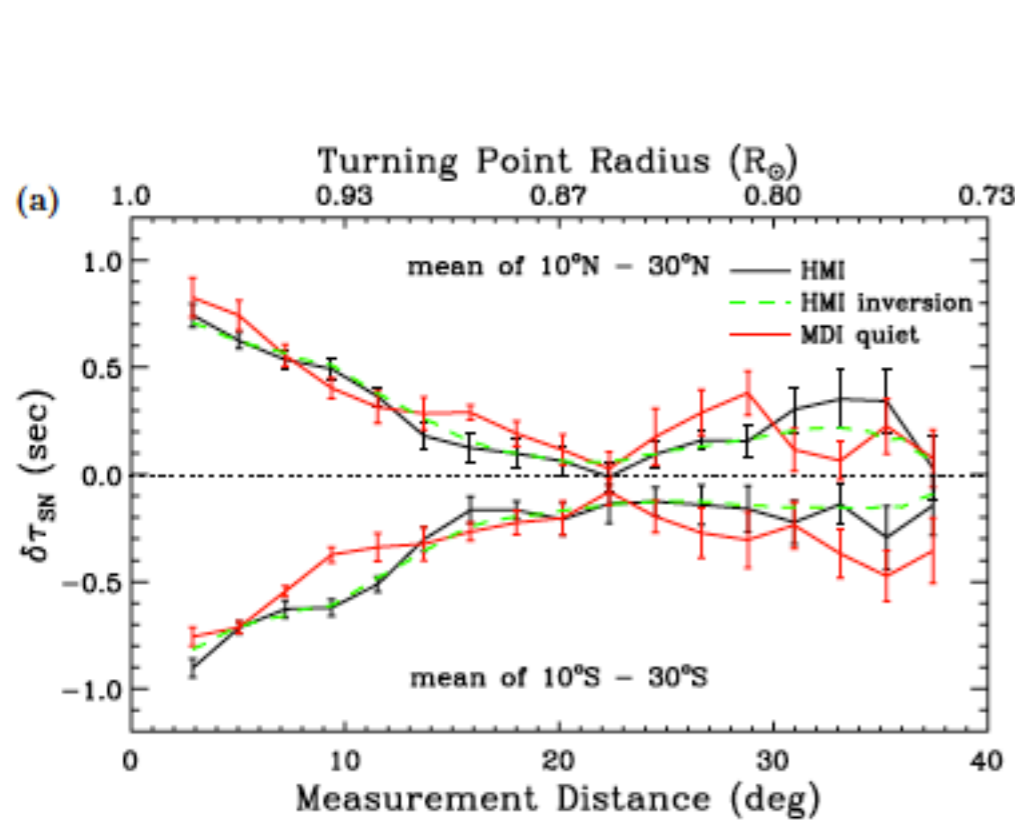


Figure 2. Top: averaged curves of latitude-dependent τ_{NS} , obtained from different HMI observables and for different measurement distances. Middle: averaged curves of longitude-dependent τ_{WE} , obtained from different observables and for different measurement distances. Bottom: differences of τ_{NS} and τ_{WE} . Note that the vertical scales for the upper two rows are different from those for the bottom row.

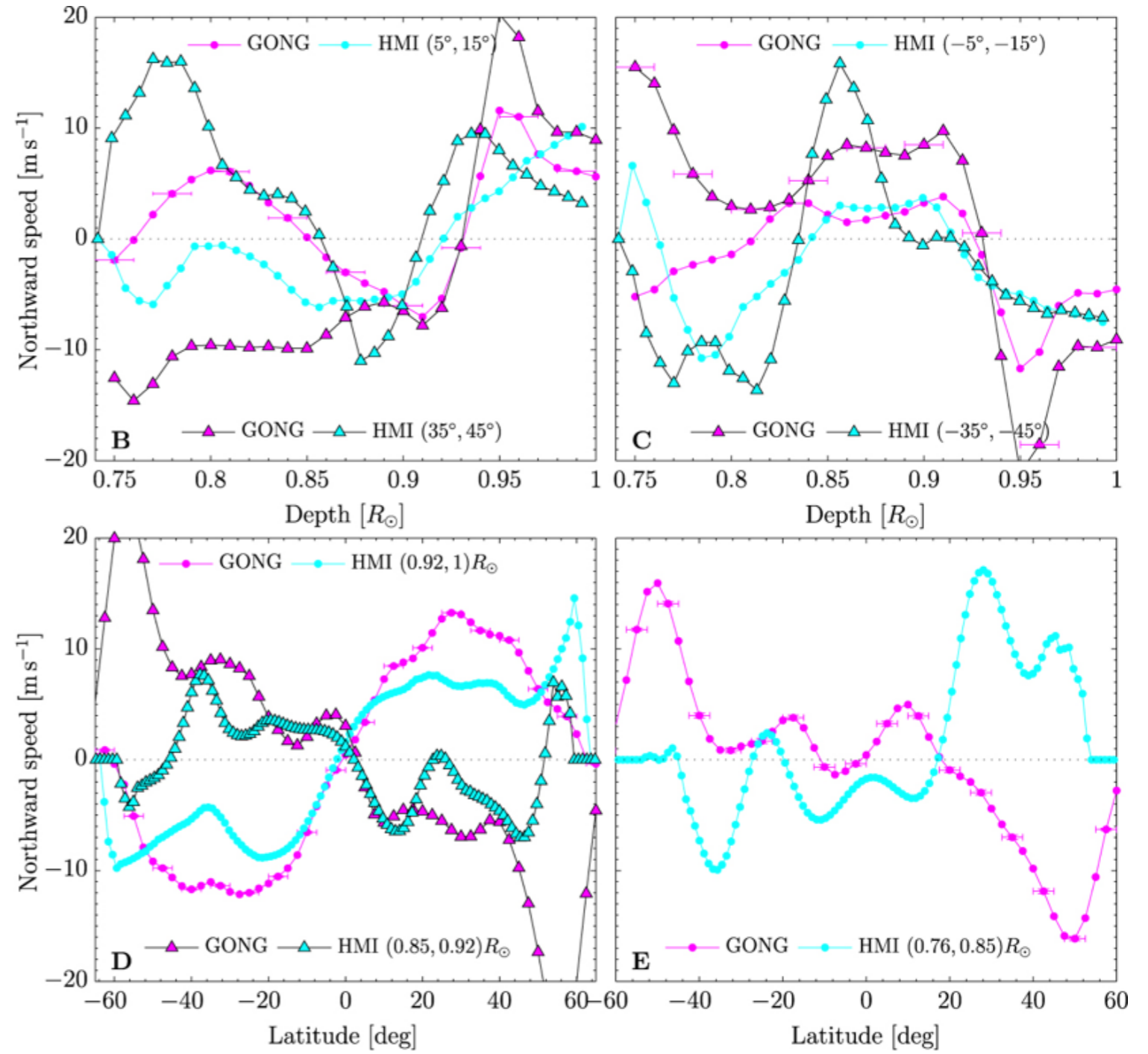
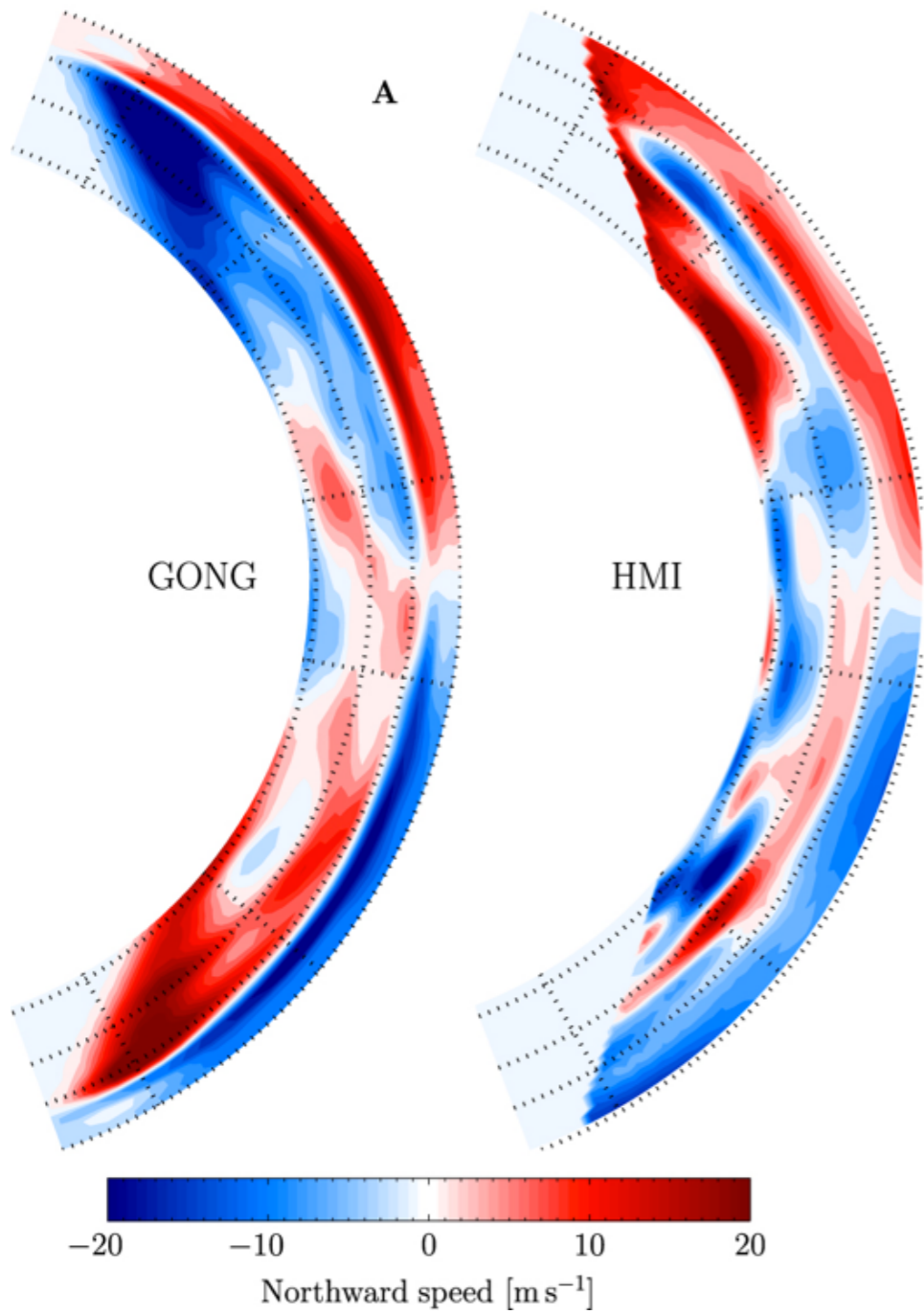
(A color version of this figure is available in the online journal.)

Shallow return-flow and double-cell signature after removing CTL systematics.

Zhao et al. 2013, ApJL.

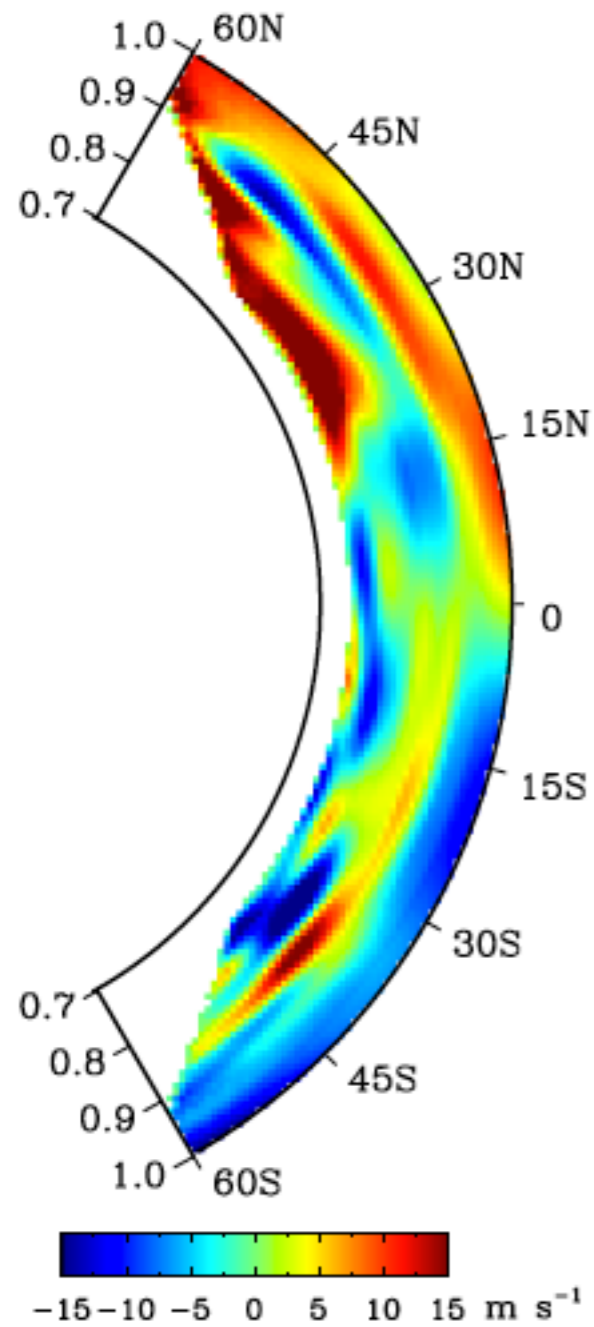


Jackiewicz et al. (2015)

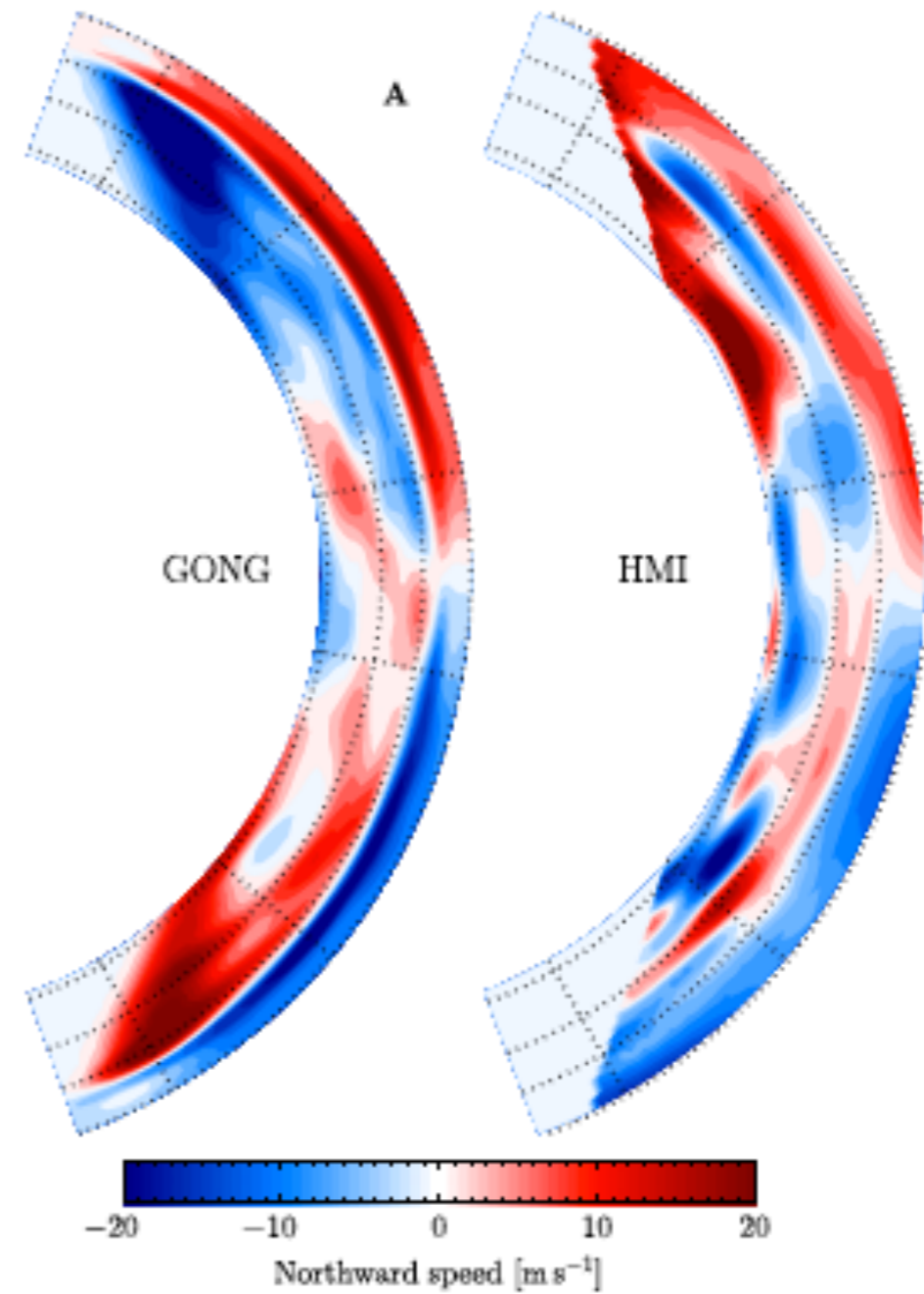


Meridional circulation without mass-conservation constraint in the inversions.

Zhao et al. 2013



Jackiewicz et al. 2015



How do flux transport dynamos work in multi-cellular MC?

IS A DEEP ONE-CELL MERIDIONAL CIRCULATION ESSENTIAL FOR THE FLUX TRANSPORT SOLAR DYNAMO?

GOPAL HAZRA^{1,2}, BIDYA BINAY KARAK^{1,3}, AND ARNAB RAI CHOUDHURI¹

¹ Department of Physics, Indian Institute of Science, Bangalore 560012, India; ghazra@physics.iisc.ernet.in

² Indian Institute of Astrophysics, Bangalore 560034, India

³ Nordita KTH Royal Institute of Technology and Stockholm University, Roslagstullsbacken 23, SE-106 91 Stockholm, Sweden

Received 2013 September 10; accepted 2013 December 17; published 2014 February 3

THE MEAN-FIELD SOLAR DYNAMO WITH A DOUBLE CELL MERIDIONAL CIRCULATION PATTERN

V. V. PIPIN^{1,2,3} AND A. G. KOSOVICHEV³

¹ Institute of Solar-Terrestrial Physics, Russian Academy of Sciences, Irkutsk, 664033, Russia

² Institute of Geophysics and Planetary Physics, UCLA, Los Angeles, CA 90065, USA

³ Hansen Experimental Physics Laboratory, Stanford University, Stanford, CA 94305, USA

Received 2013 May 21; accepted 2013 August 10; published 2013 September 24

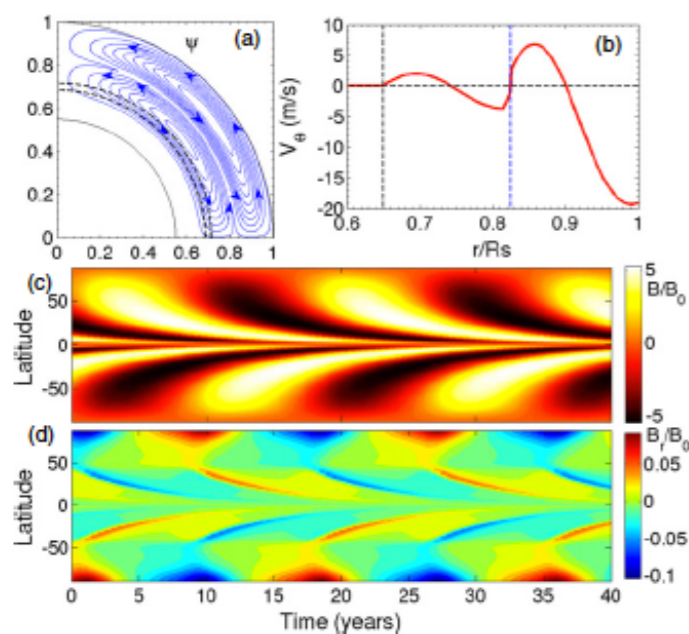


Figure 2. (a) Streamlines for two radially stacked cells of meridional circulation. Arrows show the direction of the flow. (b), (c), and (d) are the same plots as in Figure 1 for this meridional circulation.

(A color version of this figure is available in the online journal.)

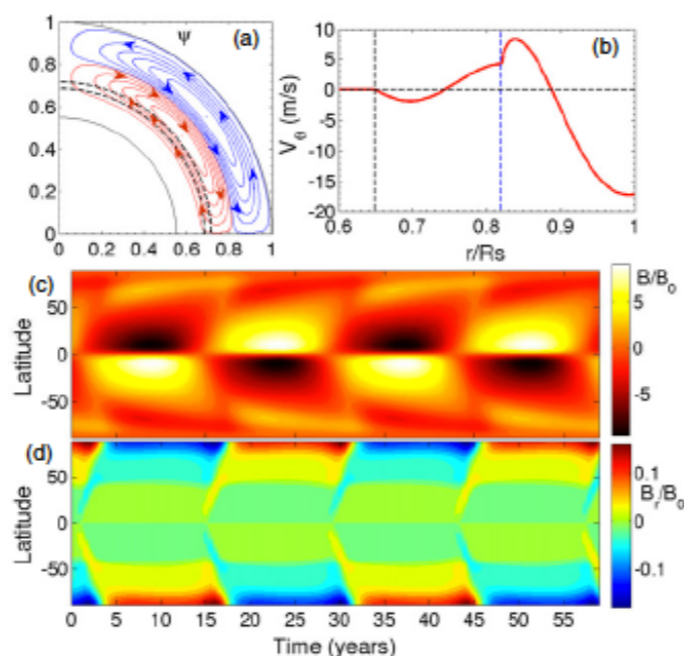


Figure 3. (a) Streamlines for two radially stacked cells of meridional circulation with circulations in the opposite sense. Arrows show the direction of the flow. (b), (c), and (d) are the same plots as in Figure 1 for this meridional circulation.

(A color version of this figure is available in the online journal.)

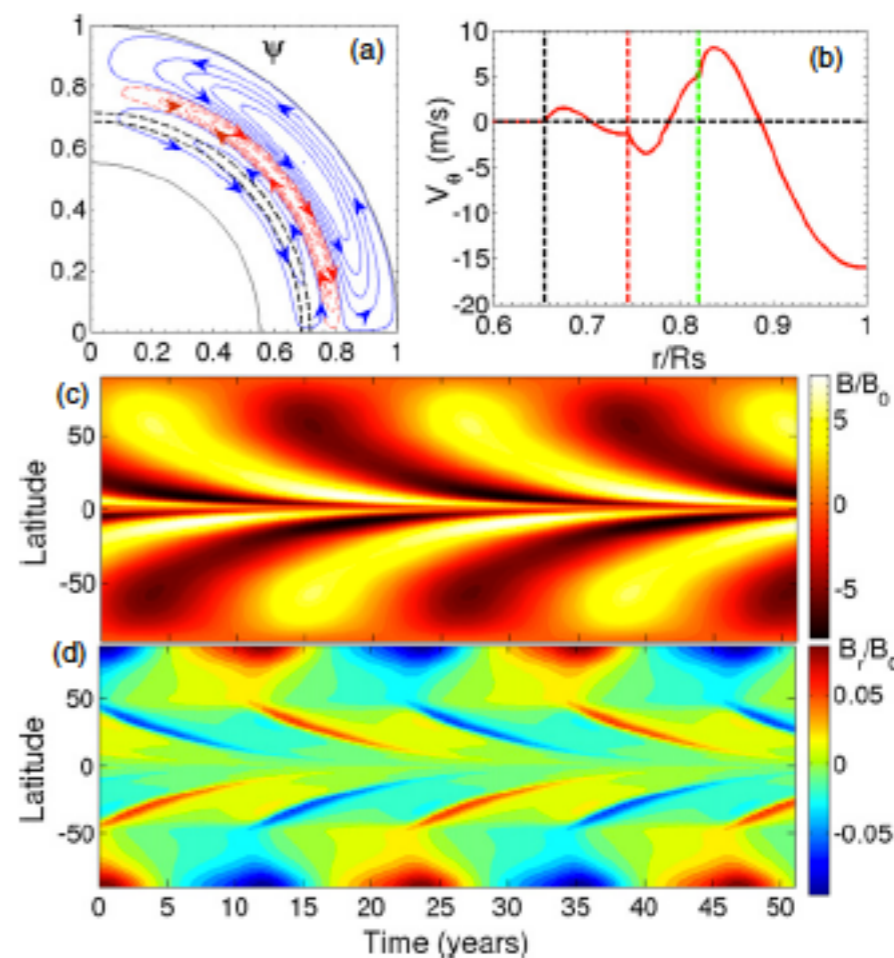
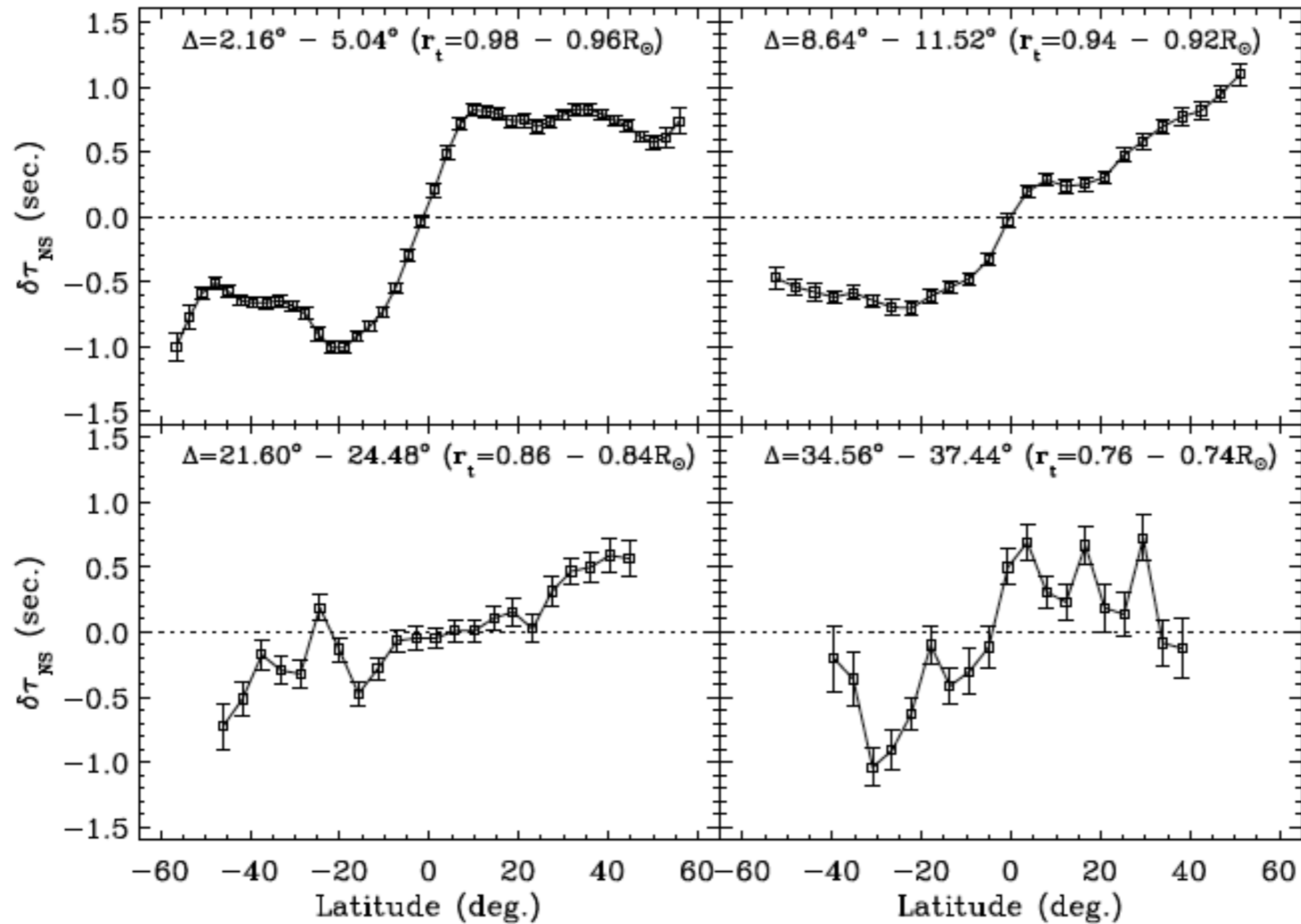
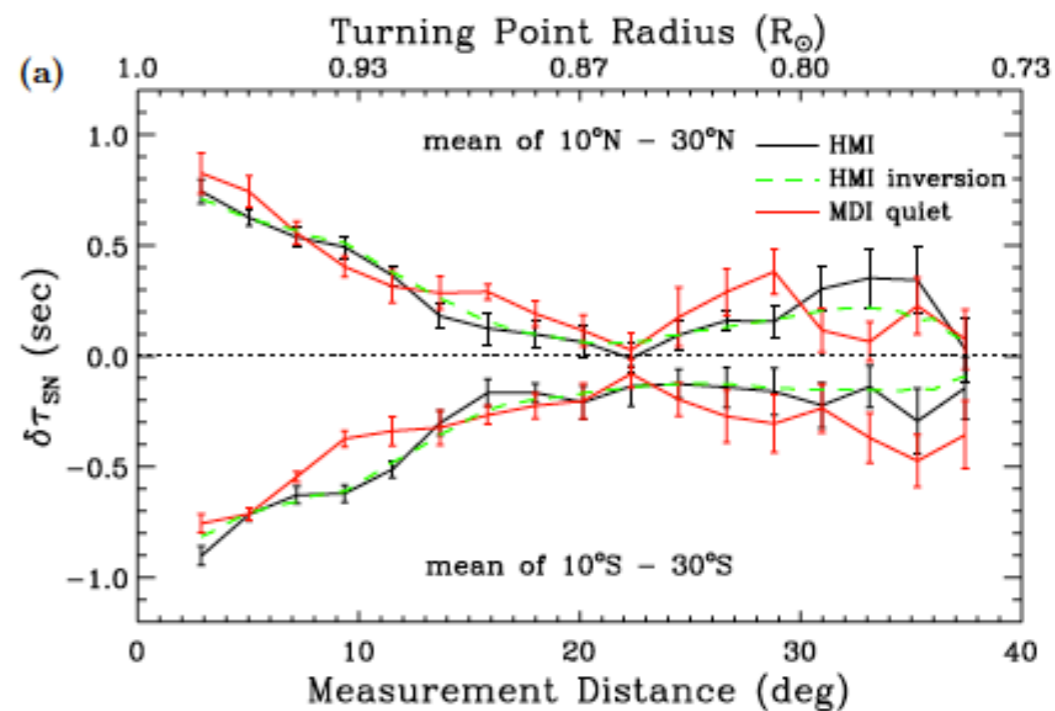
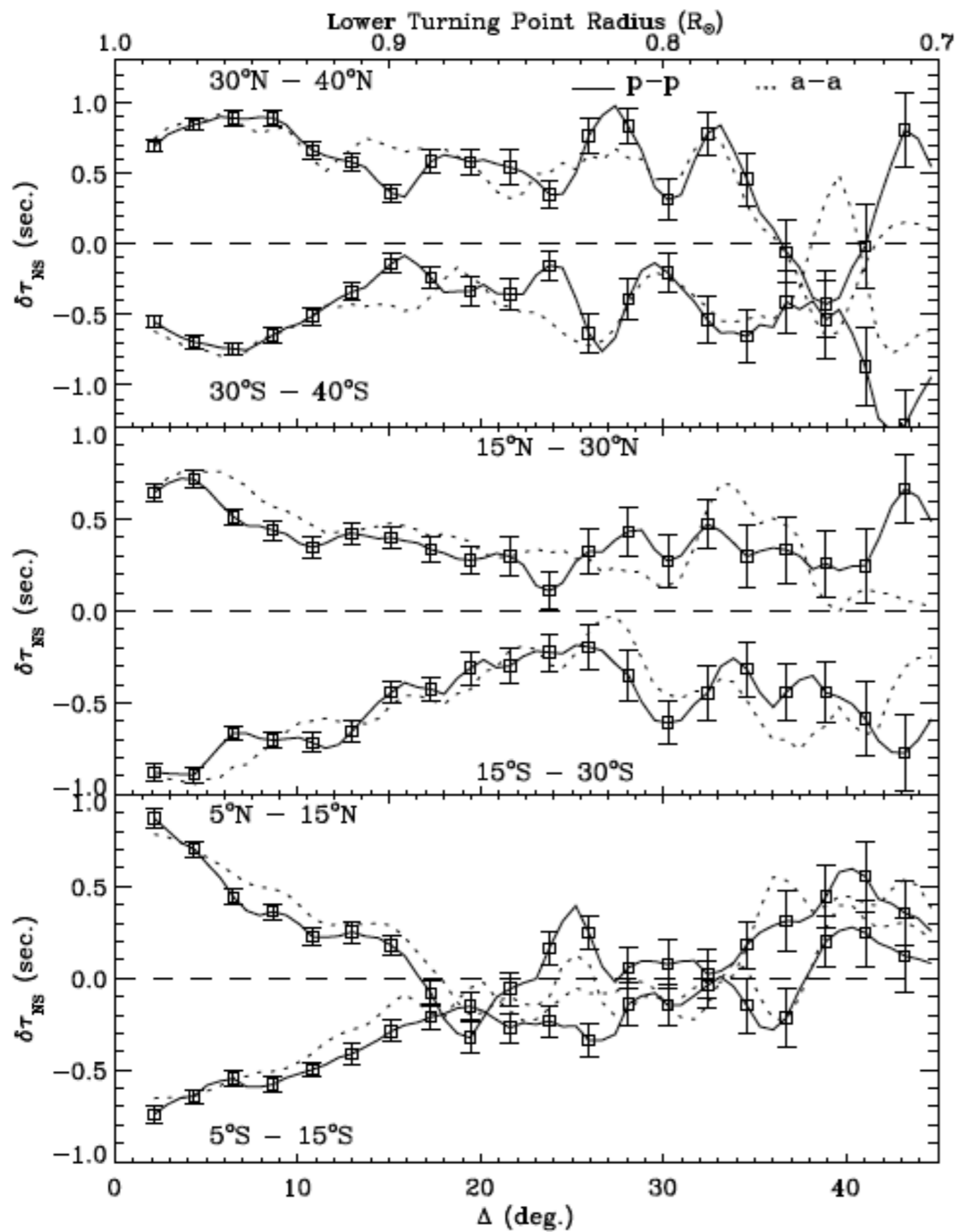


Figure 4. (a) Streamlines for three radially stacked cells of meridional circulation. Directions are shown by arrows. (b), (c), and (d) are the same plots as in Figure 1 for this meridional circulation.

Travel-time differences from 4 years of HMI data

Rajaguru and Antia (2015 ApJ)





Meridional flows with mass-conservation constraints in the inversions of travel times

$$\delta\tau = -2 \int_{\Gamma_0} \frac{\mathbf{u} \cdot \hat{\mathbf{n}}}{c^2} ds, \quad (1)$$

The solutions here are obtained by fitting stream functions satisfying mass conservation while inverting the travel times.

$$\begin{aligned} \rho u_r &= \frac{1}{r} \frac{\partial \psi}{\partial \theta} + \frac{\cos \theta}{r \sin \theta} \psi, \\ \rho u_\theta &= -\frac{\partial \psi}{\partial r} - \frac{\psi}{r}, \end{aligned}$$

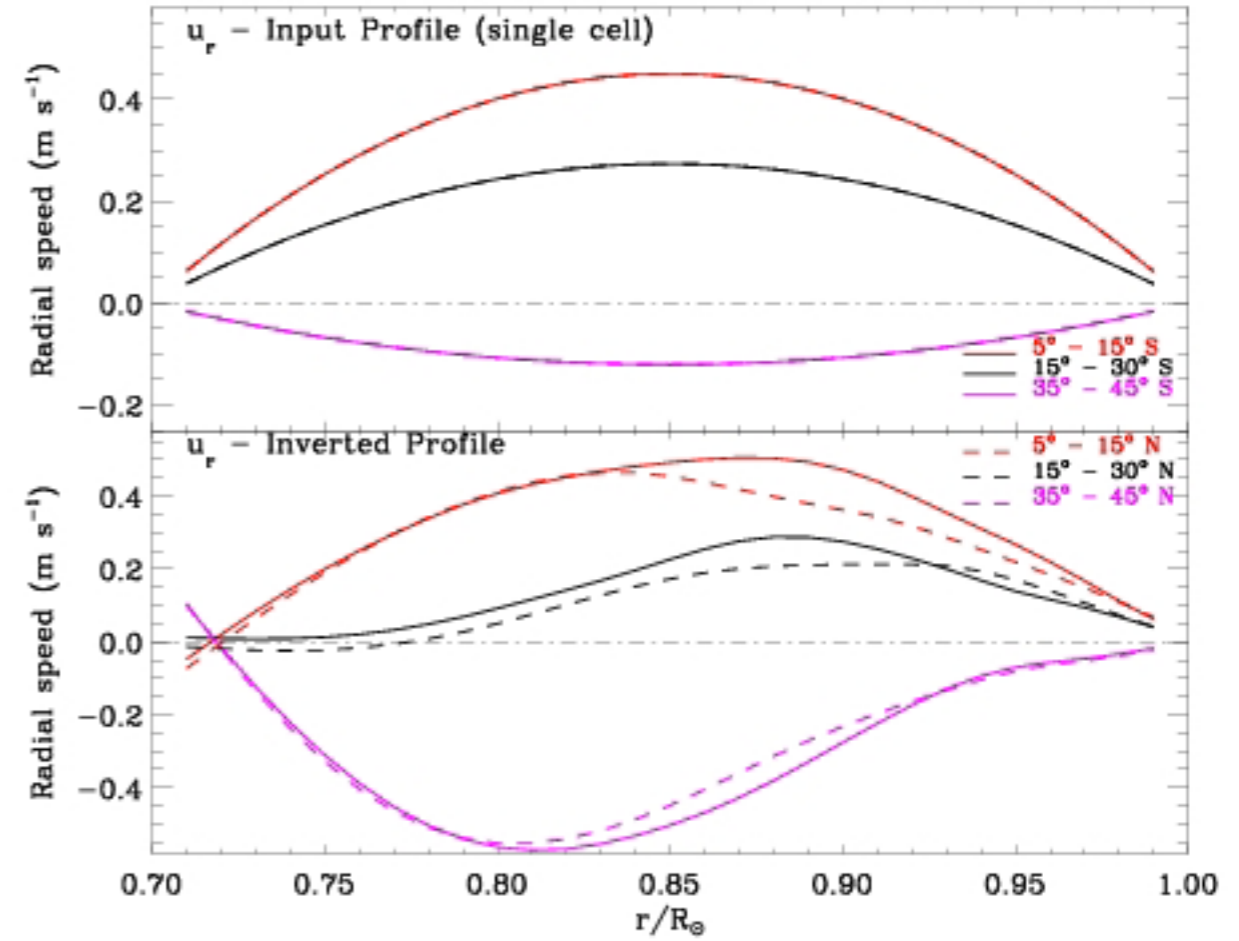
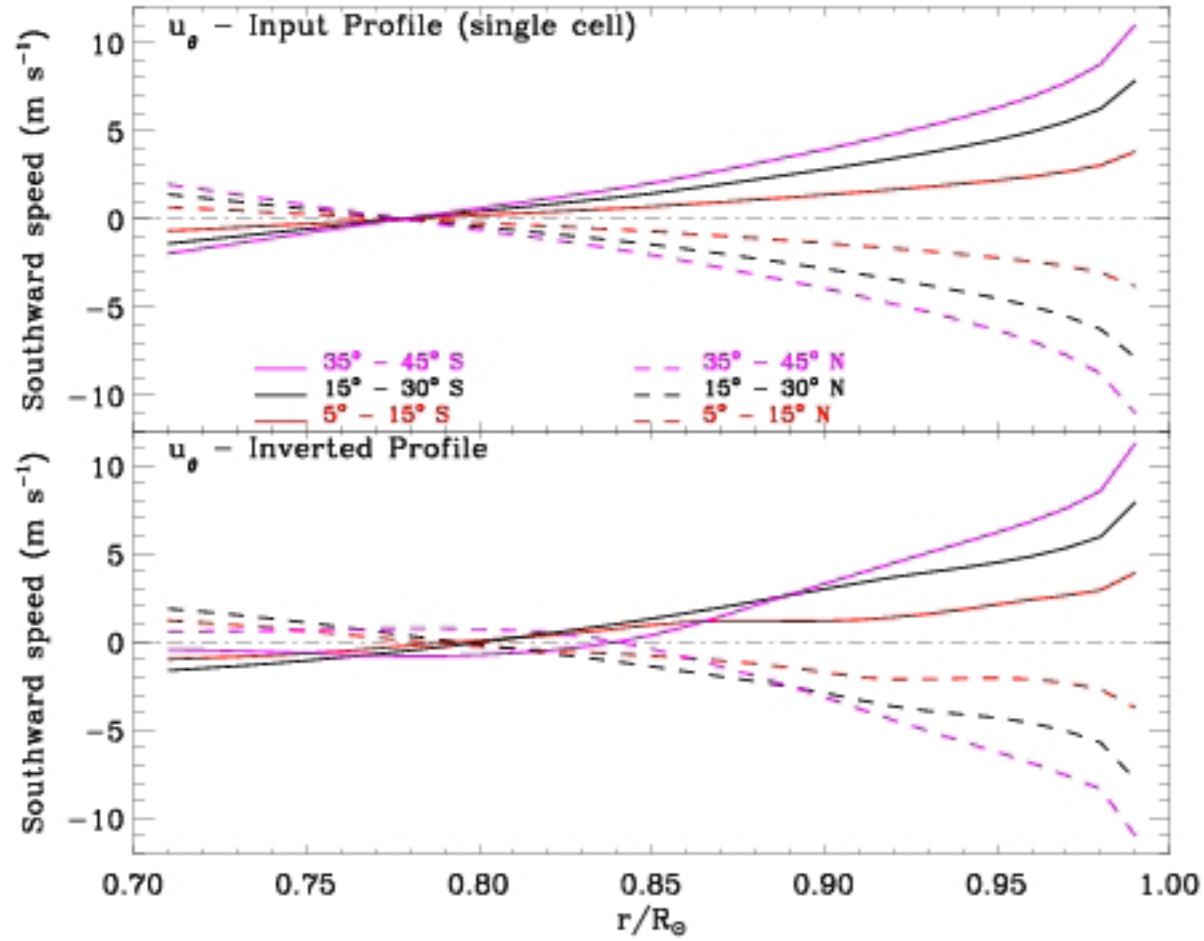
$$\psi'(r, \theta) = \sum_i \sum_j a_{ij} \Phi_i^r(r) \Phi_j^\theta(\theta), \quad \psi' = \psi / \rho$$

where $\Phi_i^r(r)$ are the cubic B-spline basis covering $0.7R_\odot \leq r \leq R_\odot$ and $\Phi_j^\theta(\theta)$ are the cubic B-spline basis covering $|\theta - \pi/2| \leq 1.055$. We use 38 knots in r which are uniformly spaced in acoustic depth and 31 knots in θ which are uniformly spaced in θ to define the B-spline

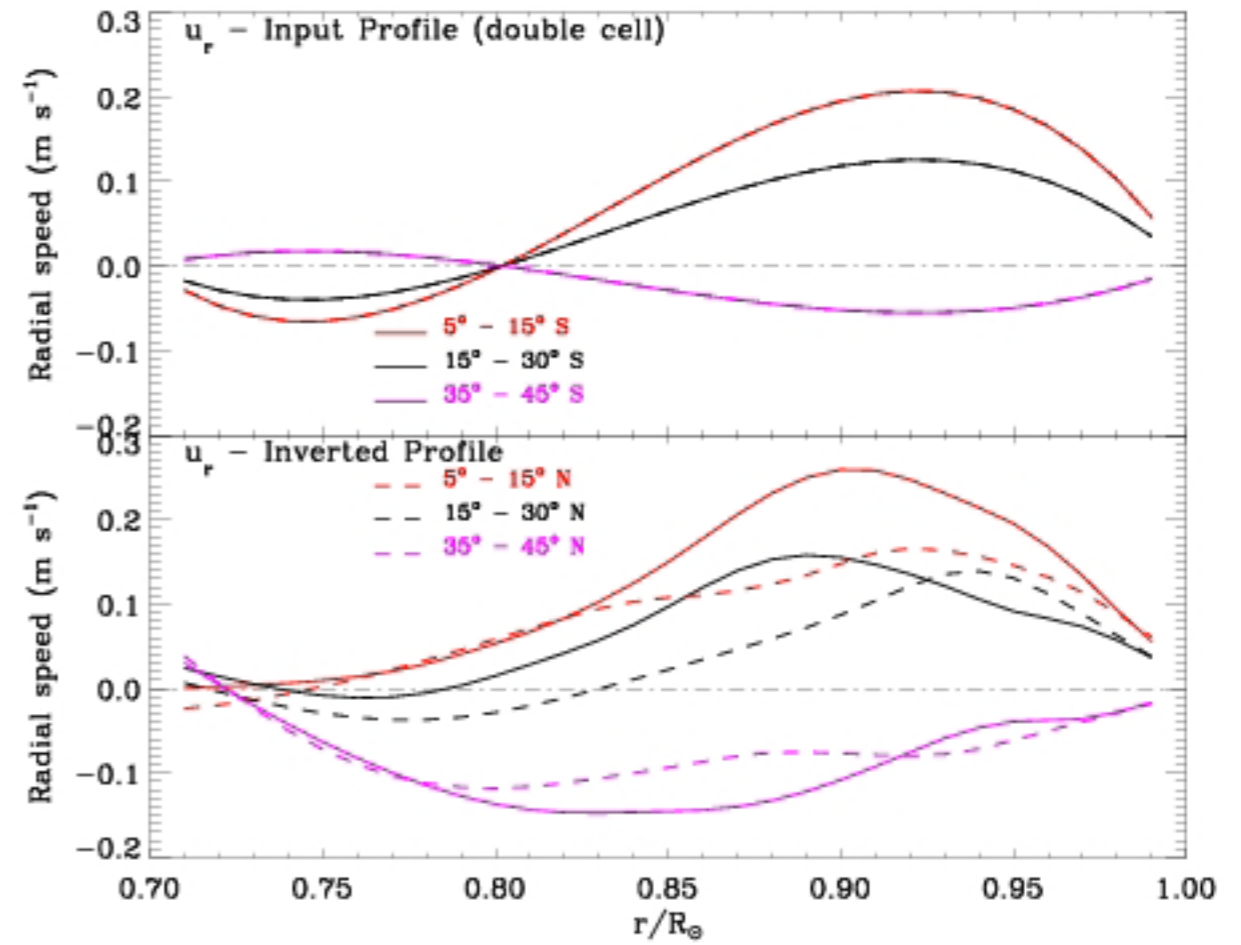
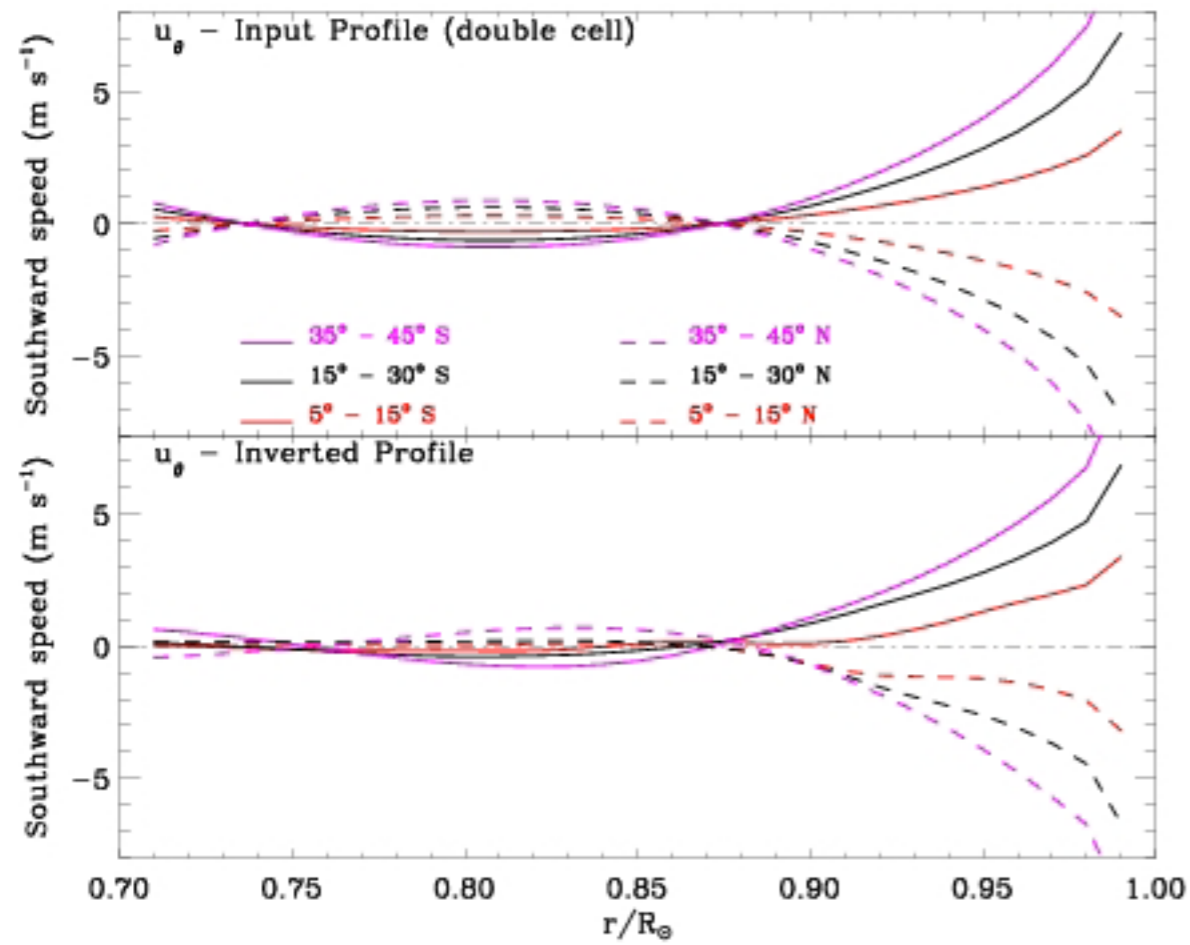
The coefficients a_{ij} determined using RLS with second derivative smoothing in both r and θ by minimizing

$$\sum_i \left(\frac{d_i}{\sigma_i} \right)^2 + \lambda_r^2 \sum \left(\frac{\partial^2 \psi'}{\partial r^2} \right)^2 + \lambda_\theta^2 \sum \left(\frac{\partial^2 \psi'}{\partial \theta^2} \right)^2$$

d_i are the residuals in the fit to eqn.(1) and σ_i are the corresponding errors in the travel-time differences. λ_r and λ_θ are the two smoothing parameters.



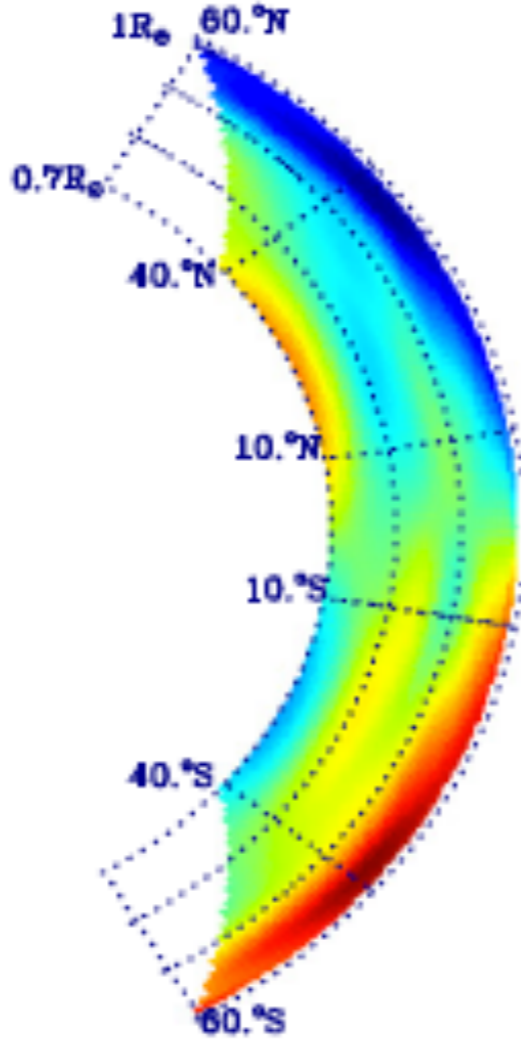
Single cell test profile (Rajaguru & Antia 2015)



Double cell test profile (Rajaguru & Antia 2015)

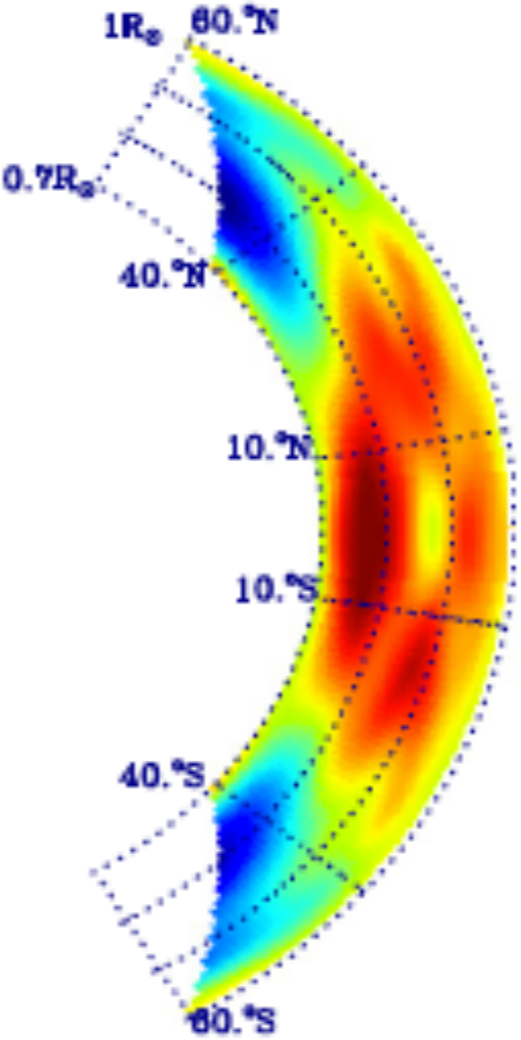
A solution with higher smoothing and lower errors.

U_θ



Southward speed (m s^{-1})
-15.00 -9.10 -3.20 2.70 8.60 14.50

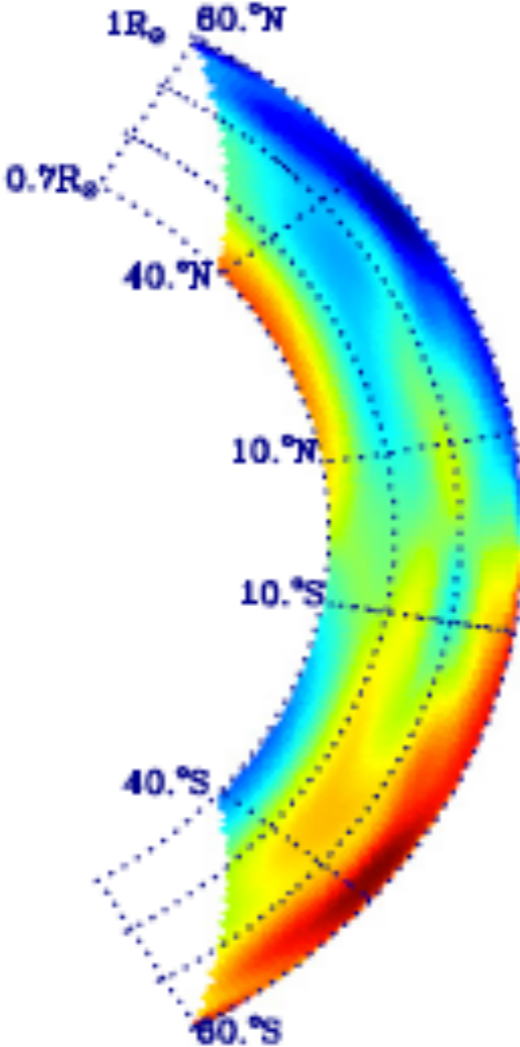
U_r



Radial speed (m s^{-1})
-1.70 -1.14 -0.58 -0.02 0.54 1.10

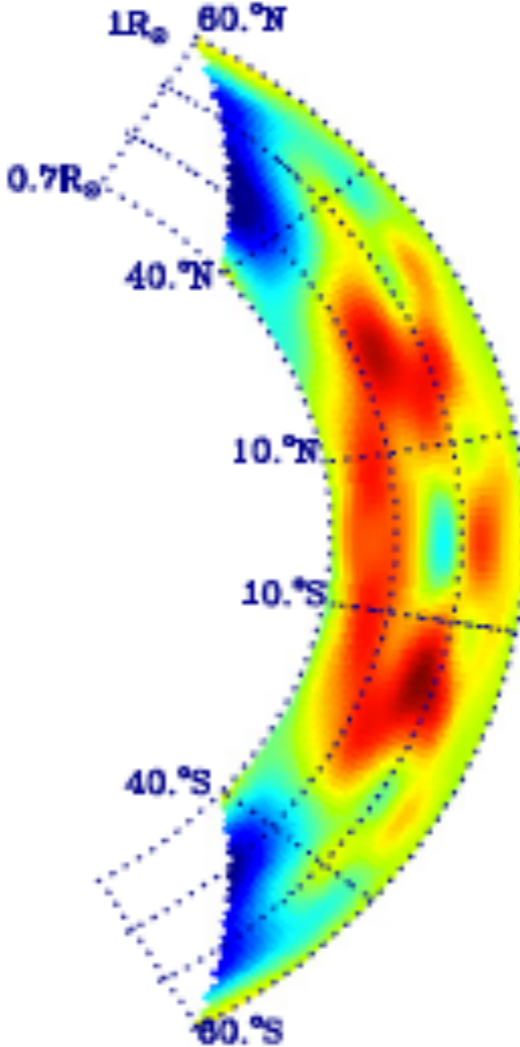
A solution with lower smoothing and slightly larger errors.

U_θ



Southward speed (m s^{-1})
-16.00 -9.80 -3.60 2.60 8.80 15.00

U_r

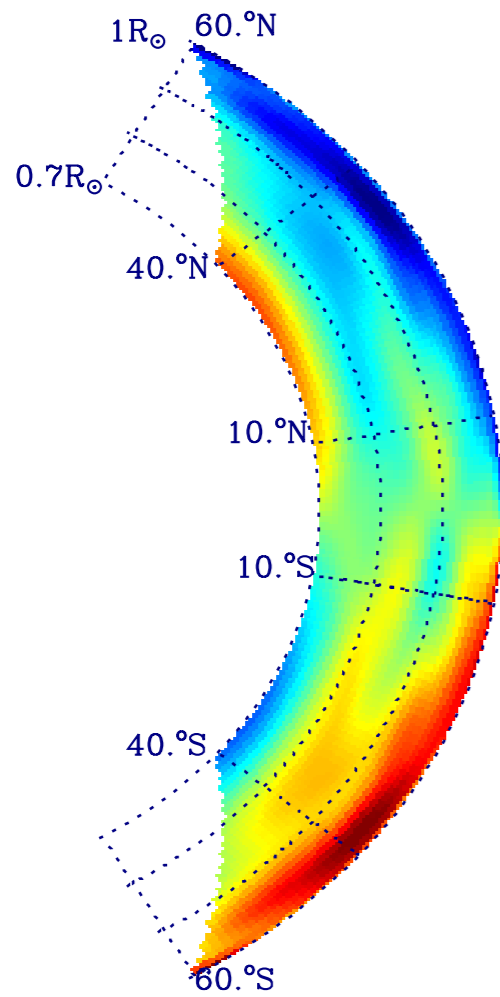


Radial speed (m s^{-1})
-2.00 -1.30 -0.60 0.10 0.80 1.50

Inverted Meridional Circulation

Rajaguru and Antia (2015)

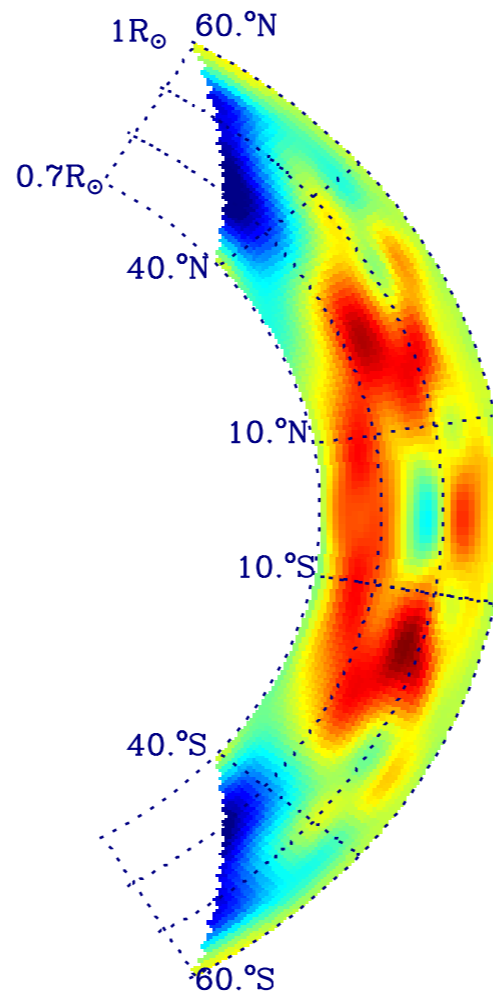
U_θ



Southward speed (m s^{-1})

-16.00 -9.80 -3.60 2.60 8.80 15.00

U_r

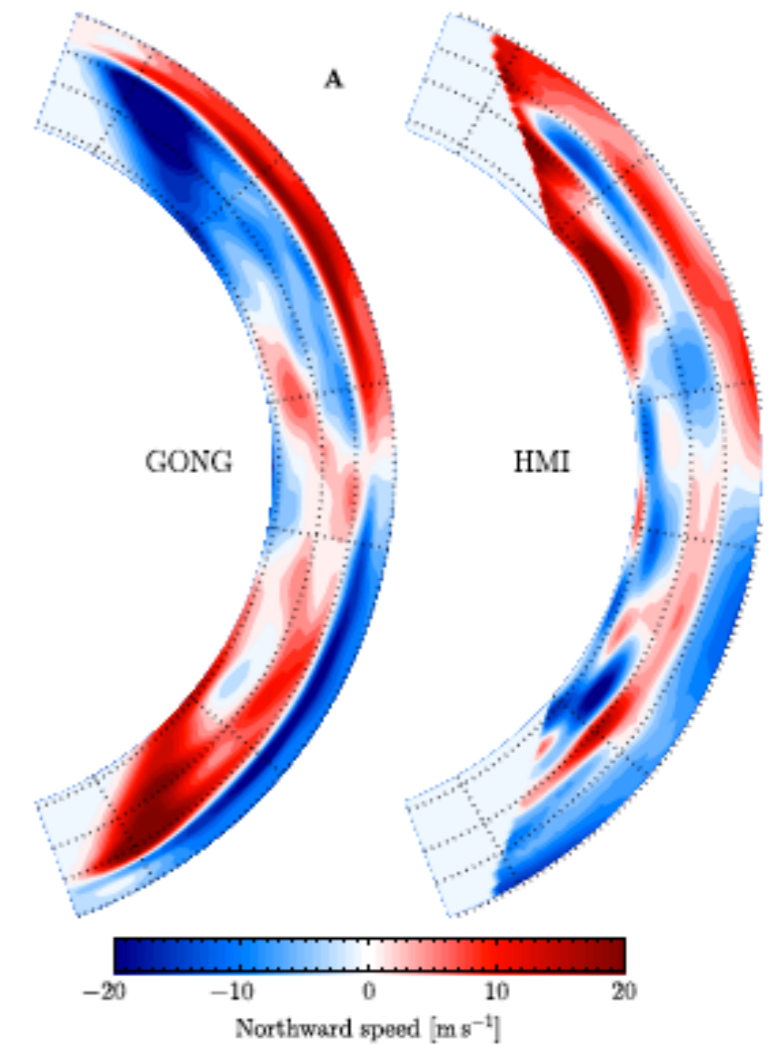


Radial speed (m s^{-1})

-2.00 -1.30 -0.60 0.10 0.80 1.50

Jackiewicz et al. (2015)

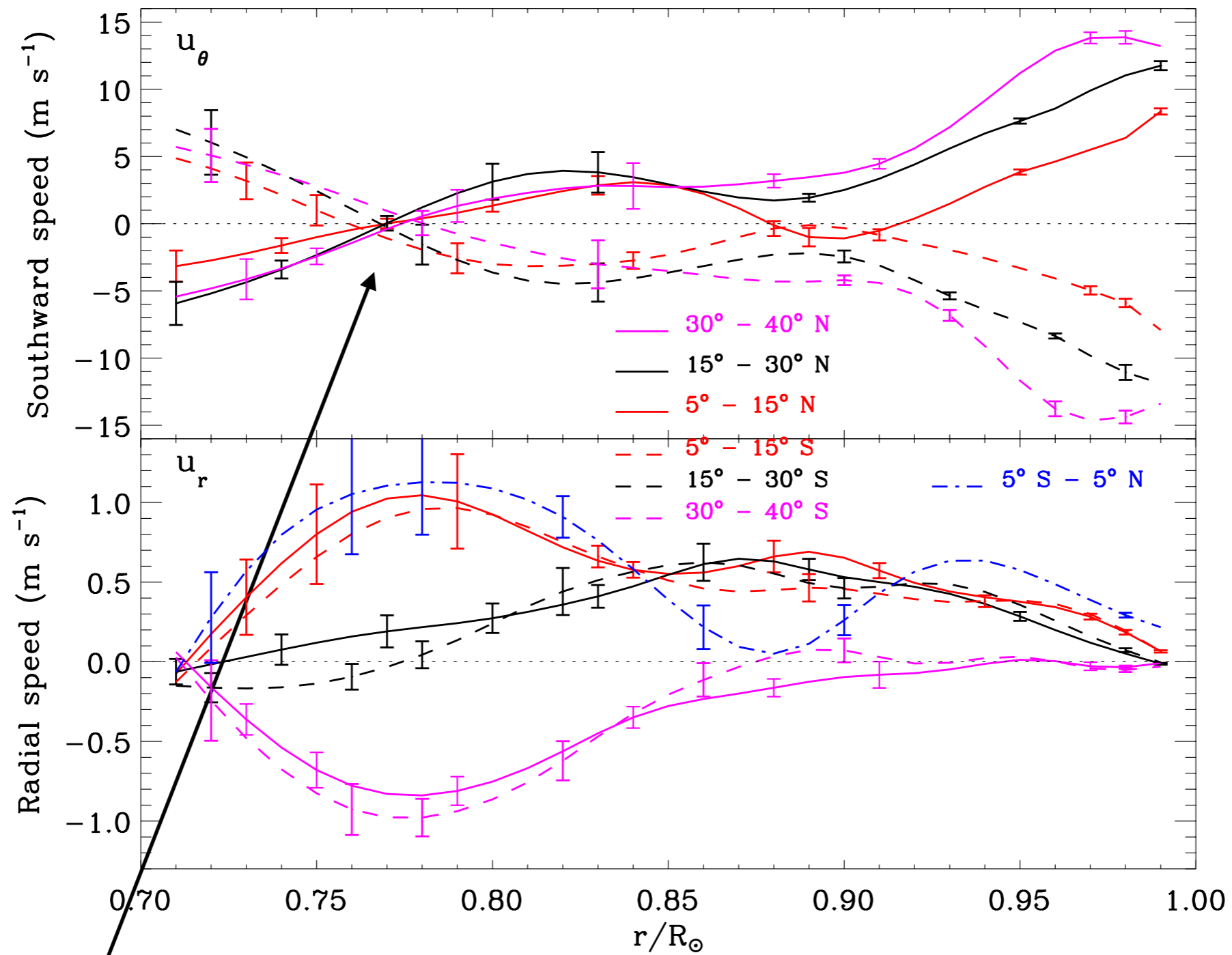
U_θ



-20 -10 0 10 20
Northward speed [m s^{-1}]

with mass-conservation constraints in the inversions

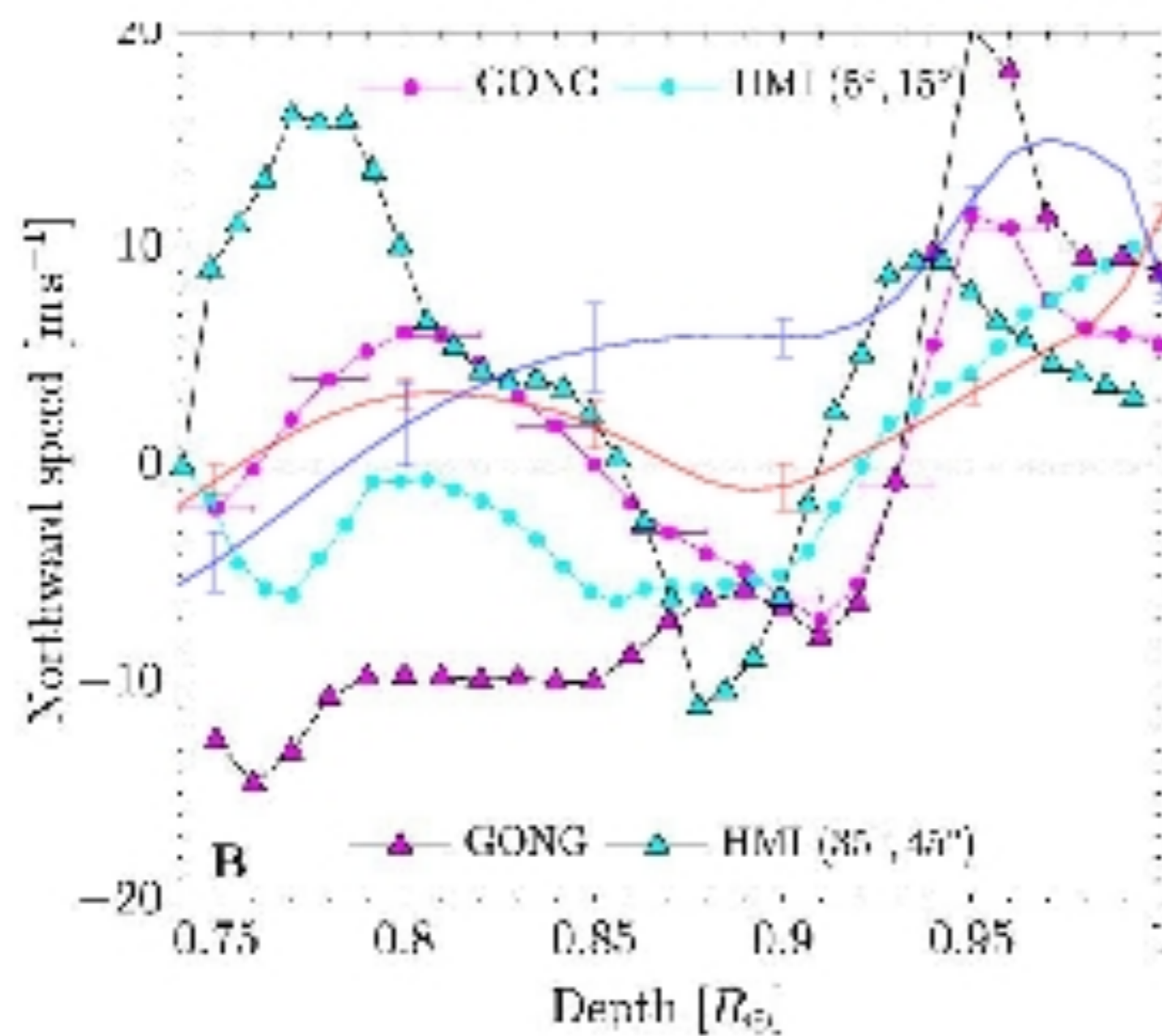
without mass-conservation constraint in the inversions



Likely reversal of flow at about $0.77 R_{\text{sun}}$.

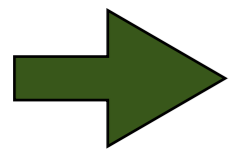
Hints of flow reversals at about $0.89 R_{\text{sun}}$ are not significant.

A single cell of meridional flow with return flow at about $0.77 R_{\text{sun}}$ is consistent with the above inversions.



Reasons for the differences between inferences on the deep structure of MC:

- (1) mass-conservation constraints
- (2) differences in inversion strategy -- sensitivity to errors and systematics in measurements.



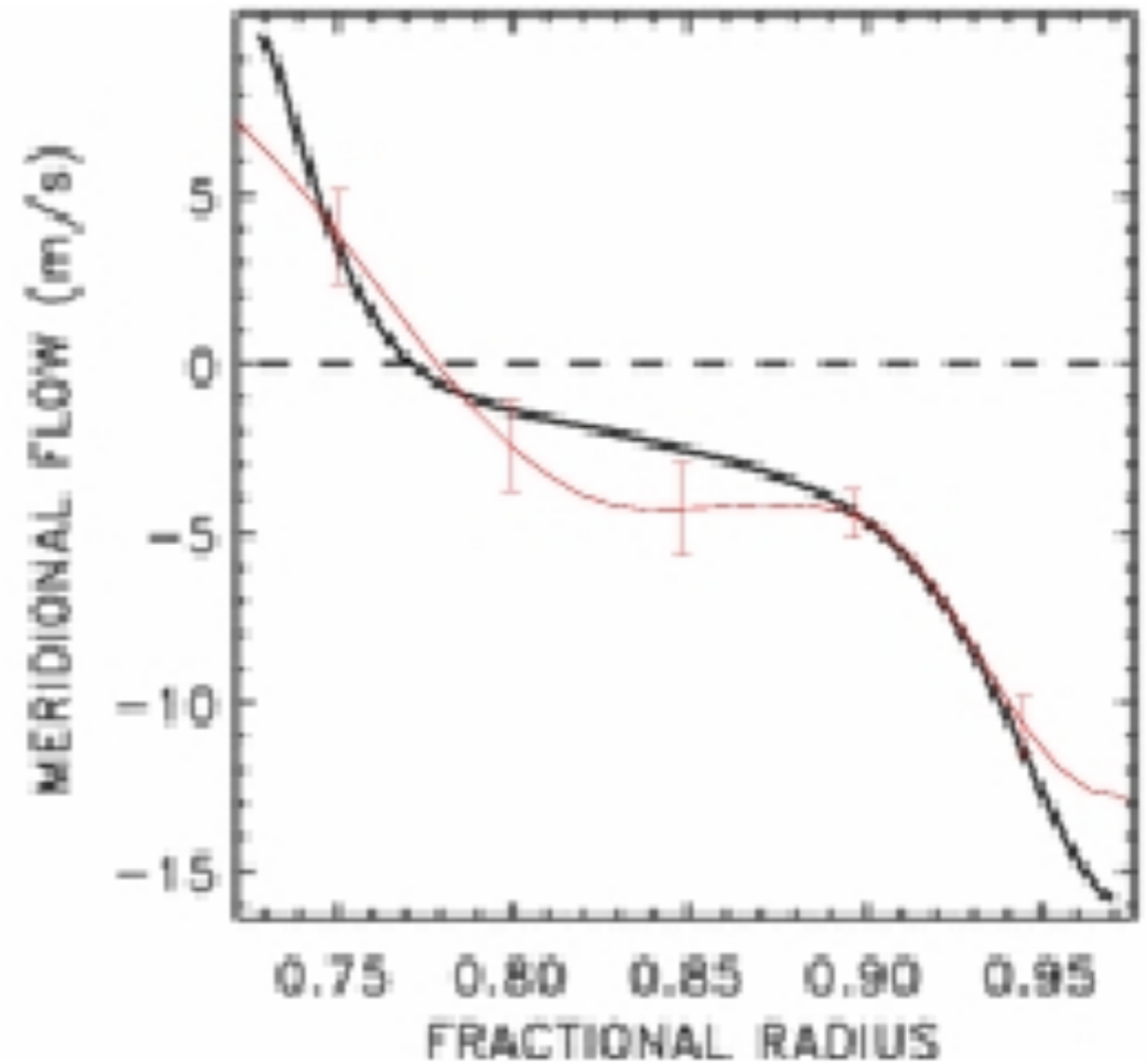
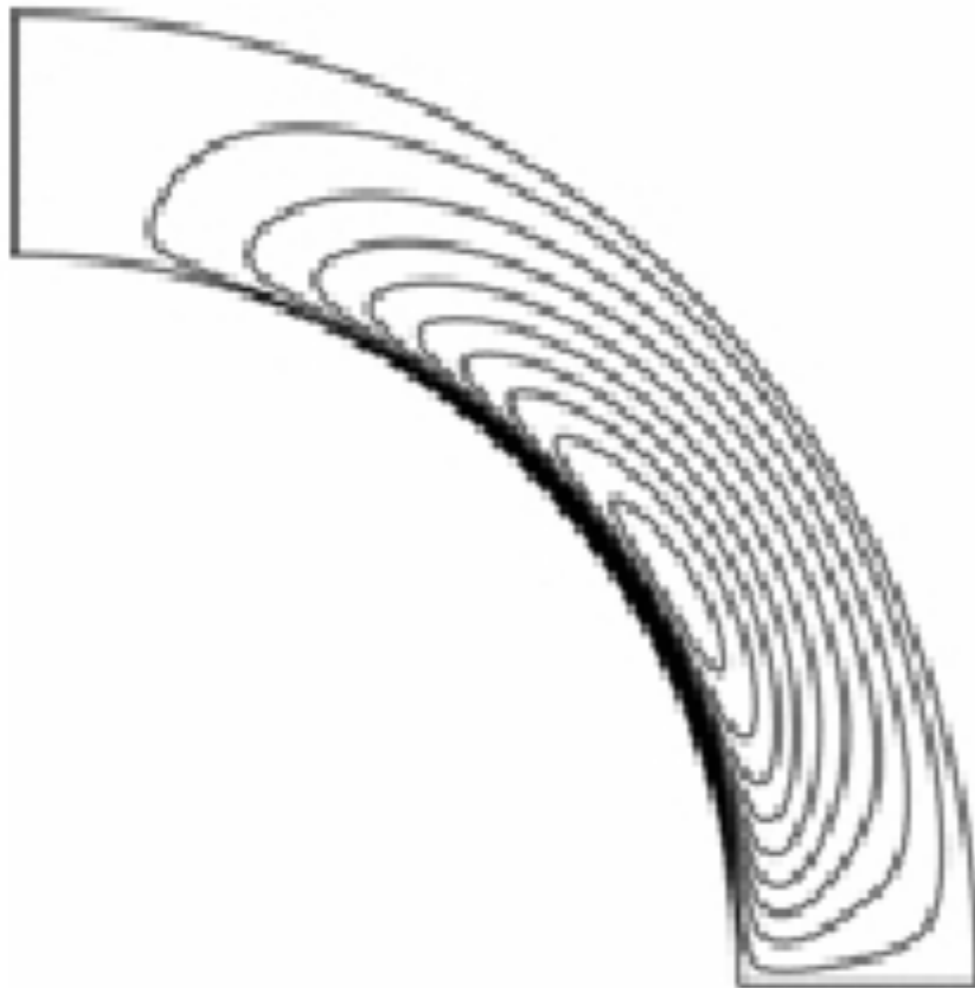
Significant improvements are needed to address the noise and systematics.

Differential rotation of main-sequence dwarfs and its dynamo efficiency

L. L. Kitchatinov^{1,2★} and S. V. Olemskoy¹

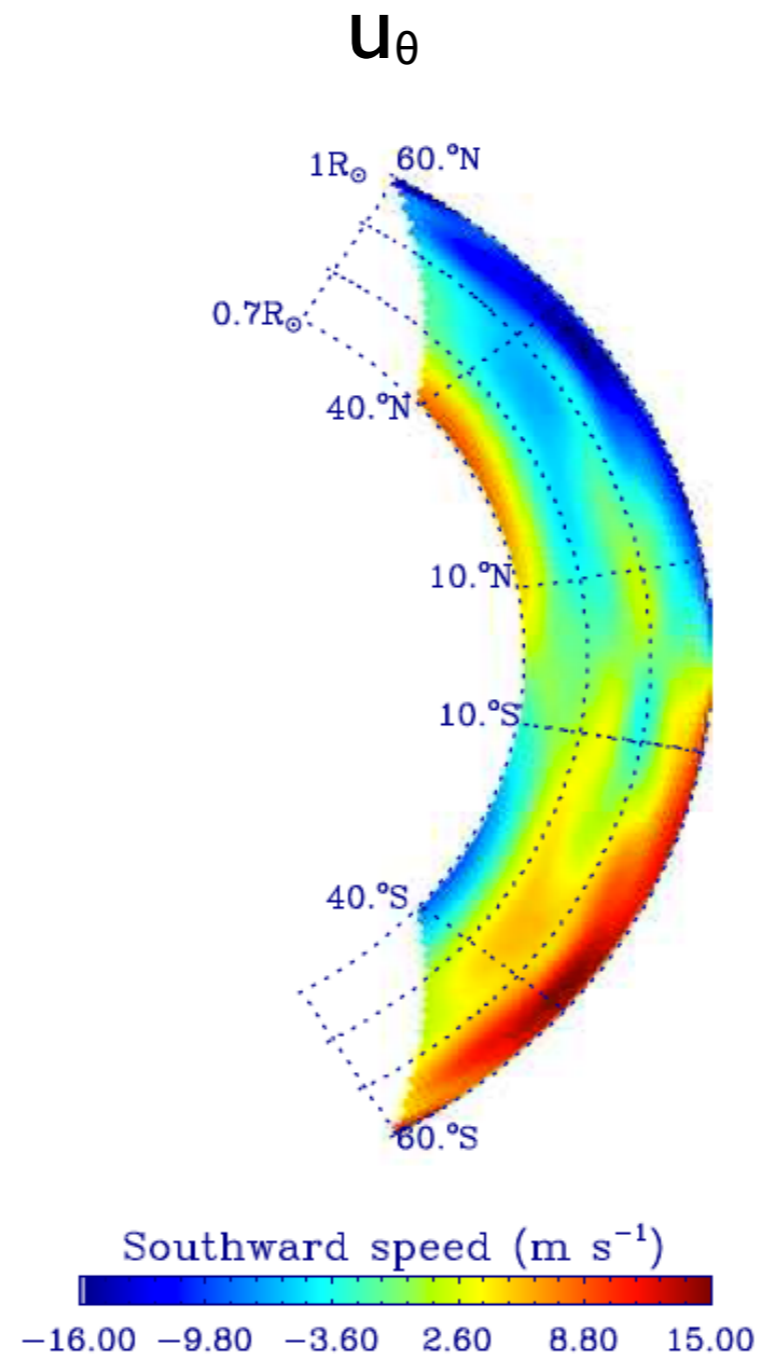
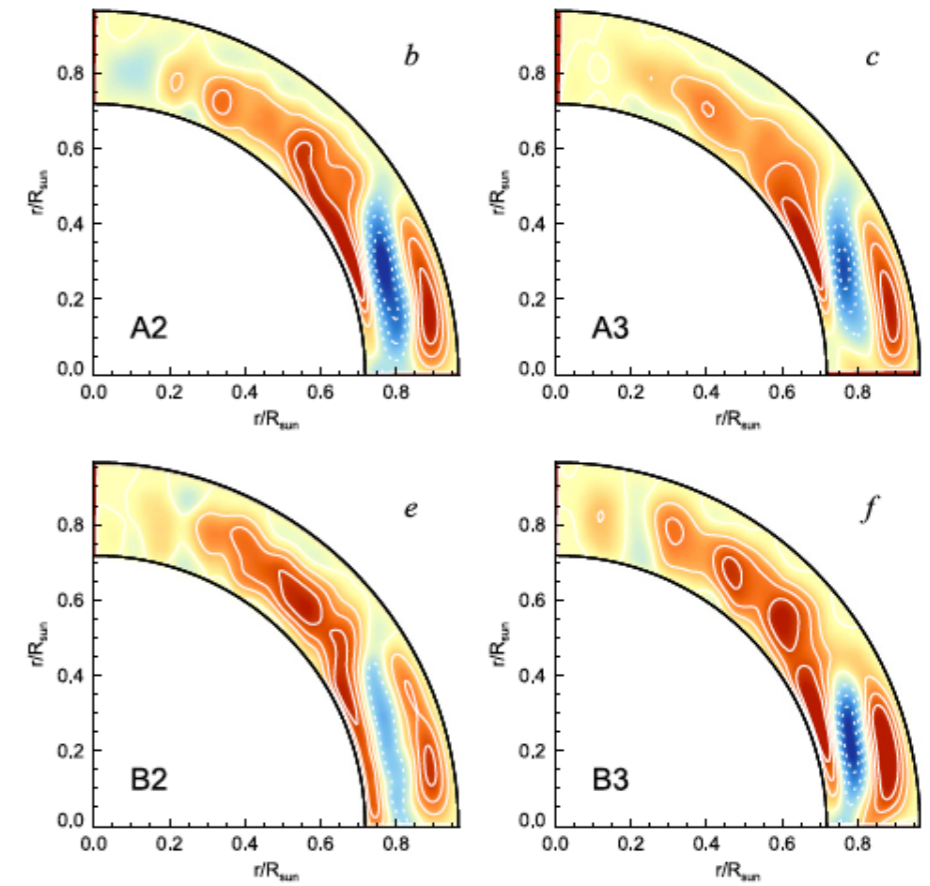
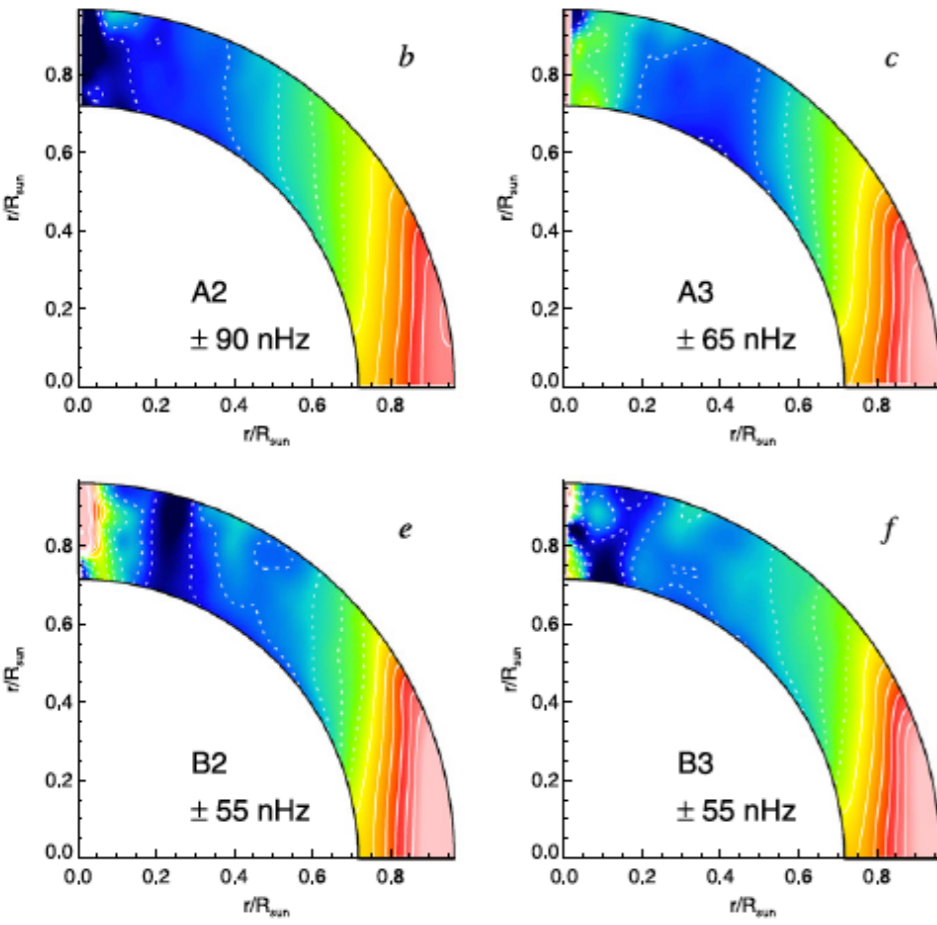
¹*Institute for Solar-Terrestrial Physics, PO Box 291, Irkutsk 664033, Russia*

²*Pulkovo Astronomical Observatory, St. Petersburg 196140, Russia*



Numerical models of differential rotation and MC

Featherstone & Miesch (2015)



Main inferences:

- (1) Within errors, the measurements are consistent with a single deep cell of MC
 - return-flow likely below $0.77 R_{\text{sun}}$
 - broad upwellings near the equatorial regions ($10^{\circ}\text{S} - 10^{\circ}\text{N}$) with radial speeds of ~ 1 m/sec over the depth ranges of $0.7 - 0.8 R_{\text{sun}}$ and $0.9 - 0.97 R_{\text{sun}}$
- (2) There are signatures of multi-cellular structure at low latitudes (< 25 deg.) but the signals are close to error limits.

What next?

1. Understand the Centre-to-Limb Systematics – devise new correction strategies
2. Improve S/N in measurements – use longer data sets
3. Closer exchange between researchers and concerted efforts to understand the differences in methods of analyses and results.

Thank you! .